IRSN
INSTITUT
DE RADIOPROTECTION
ET DE SÛRETÉ NUCLÉAIRE

Report on the IRSN's investigations following the widespread detection of ^{106}Ru in Europe early October 2017

January 2018

1) Introduction

Ruthenium-106 (^{106}Ru) is an anthropogenic radionuclide which is usually not observed in the atmosphere. Early October 2017, it was detected in almost all European countries. Observed activities ranged from a few µBq/m^3 to about 150 mBq/m^3. Although, these concentrations did not pose any health or environmental issues, this widespread detection suggested that the source-term must have been quite high. Taken into account all these elements, IRSN decided to perform further investigations in order (1) to identify the possible location of the source, 2) to assess the total activity released and the release duration and 3) to understand the process that could be at the origin of the release of ^{106}Ru alone.

The present report summarizes the main results of these investigations.

2) Main characteristics of ^{106}Ru

Physical characteristics

Ruthenium is a transition metal that is part of the platinum group with iridium, osmium and rhodium. In metallic form, it does not react with acids, water or air. This chemical element is extremely volatile and reacts with sulphides, ethanol, coal …

^{106}Ru is a radionuclide of artificial origin. It is a fission product from the nuclear industry with a radioactive half-life of 371.8 days.

By disintegrating, ^{106}Ru is transformed into rhodium 106 (^{106}Rh, half-life of 30 seconds). It is a pure beta emitter but given the very short half-life of its descendant, it is generally at radioactive equilibrium with ^{106}Rh which is an emitter of gamma radiation. Due to this

equilibrium, the quantification of ^{106}Ru activity can be easily performed by gamma spectrometry.

Behavior of ruthenium in the environment

Little information is available on the behavior of ruthenium in the environment and, more particularly, in the food chain.

To IRSN knowledge, it appears that ruthenium is a generally non-mobile element in soils, its mobility depending on its chemical form. Unlike cesium (which is a potassium analogue, essential for the biological development of plants), ruthenium is not an analogue of a biologically essential element for flora. Its uptake by plant roots is therefore very low compared to cesium or strontium. In addition, up to 99% of the total ruthenium content absorbed by the plants is retained by the root system, and only a very small amount is accumulated in the aerial mass. Of the fission products, ^{106}Ru is among the least available for uptake by plants. ^{106}Ru is thus very weakly transferred into the food chain.

Exposure routes and biological behavior of ruthenium in humans

In case of atmospheric releases, the population is susceptible to be exposed to radiation during the passage of the plume via internal contamination by inhalation and via external irradiation from radionuclides present in the air (immersion) and deposited on the soil.

After ingestion, only a fraction of ruthenium is absorbed into the digestive tract. According to the International Commission on Radiological Protection (ICRP, 1993), this fraction is about 5%, whatever the chemical form of thecompounds. The most exposed organ in case of ingestion is the colon.

In case of inhalation, the pulmonary absorption that precedes its distribution in the body depends on the physicochemical form of the compounds. The most exposed organs are in this case the colon and the lungs.

Once it has entered the body, ruthenium distributes relatively evenly in the tissues. The ICRP indicates that about 35% of absorbed activity is retained in tissues with an elimination half-life of 8 days, 30% with a biological half-life of 35 days and 20% with a biological half-life of 1,000 days. The biological half-time in body fluids is 0.3 days and it is assumed that 15% of the systemic activity is excreted directly, mainly in urinare (4 times more than by the faecal route).

Radiotoxicological properties and risk associated with ^{106}Ru

The radiological risk associated with exposure to ^{106}Ru can be estimated from dosimetric evaluations taking into account the biological behavior of the ruthenium compound under consideration and its physical emission characteristics.

In any case, the risk depends on the amount incorporated. As an indication, the effective dose received by a person (adult) who would be exposed for a whole year to ^{106}Ru present in air at a concentration of 1 Bq/m^3 would be 0.5 milli-sievert (mSv). This dose can be

compared to the dose limit of 1 mSv per year set for the population by international recommendations. Exposure to ^{106}Ru measured at low levels (up to several hundred milli-becquerels for a few days) is therefore insignificant in health terms.

3) Observations of ^{106}Ru in the atmosphere in Europe between late September and early October 2017

All European countries have networks of radioactivity monitoring stations that qualify and quantify natural and artificial radioactivity in the environment and especially in the atmosphere. These networks enabled the detection of ^{106}Ru (which is, in normal condition, not detected in the atmosphere) in Europe at the end of September 2017.

The ^{106}Ru measurements that were performed in Europe are of two types:

- in the vast majority of cases, these measurements are carried out on filters placed in air sampling stations having flow rates of between a few tens and a few hundreds of cubic meters per hour (m^3/h). These filters are taken manually at regular intervals (ranging from one day to typically one week depending on the stations or the country) and sent to radioactive metrology laboratories that quantify ^{106}Ru activity by gamma spectrometry. The interpretation of these measurements, expressed in Bq/m^3, is delicate insofar as they correspond to an integration over a period of time which can go up to several days. It is therefore important, in order to be able to compare them, to always consider the sampling period (one day, one week, ...). To illustrate this, let's consider that the atmosphere was contaminated at one point during 24 hours and that two stations, sampling 100 m^3/h of air each, were installed at this point. The filter of the first station is removed after 24 hours of contamination while the filter of the second station is removed after one week. The measurements made on the two filters will give exactly the same activity (for example 100 Bq) but once stated to the value per m^3, in the first case the final value will be 100 Bq/(24 x 100 m^3), *i.e.* 42 mBq/m^3 whereas in the second case the final value will be 100 Bq/(24 x 7 x 100 m^3) *i.e.* 5.9 mBq/m^3. The direct comparison of the values provided by the different networks is therefore only meaningful if, on the one hand, we consider the sampling duration and, on the other hand, we can estimate the duration of the air contamination during the sampling period.

- in some cases, these are measurements of ^{106}Ru deposits. These are estimated either from samples of rainwater (Bq/L) or from samples of grass (Bq/kg), or finally from smears on surfaces of standardized size (Bq/m^2). In all cases, the same precautions as those mentioned above are to be taken into account to interpret and compare these data.

Annex 1 brings together all the data provided by European countries (as well as by Ukraine and Russia) following the request made by the IAEA in early October 2017 (IAEA 2017a,

IAEA 2017b) or data published by Roshydromet[1] (Federal Service for Hydrometeorology and Environmental Monitoring of Russia).

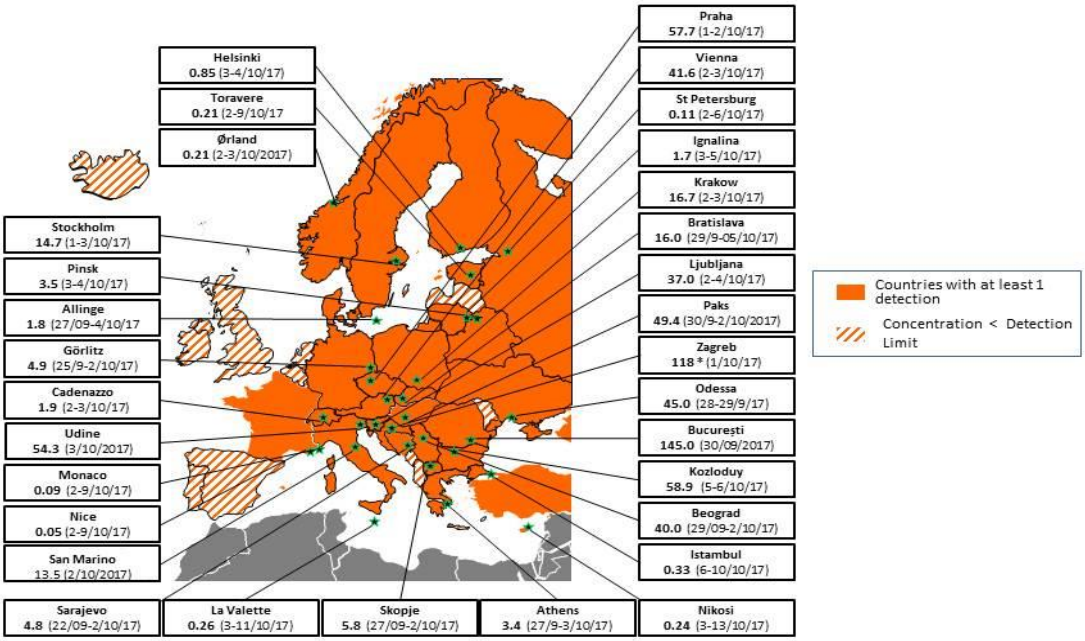

Figure 1 : Maximal atmospheric ^{106}Ru activities observed in Europe in September and October 2017. Values are given in mBq/m^3 and sampling period is specified in bracket. Values published by Roshydromet (Russia) are not indicated on this map.

Examination of these data leads to the following comments:

- ^{106}Ru was observed between the end of September and mid-October 2017 in the atmosphere of 31 countries of the European continent at levels ranging from a few µBq/m^3 to more than 140 mBq/m^3. Figure 1 shows the maximum values observed in each country. Due to the wide variation in filter sampling periods, it is not possible to directly compare the values obtained in different countries. Figure 2 presents, for each European monitoring station, the average value of the ^{106}Ru concentration in the atmosphere during the period during which ruthenium was observed ("raw data"). As mentionned earlier, for many observation points (*i.e.* stations where sampling period is longer than one day) the sampling period exceeds the time during which the ruthenium was present in the atmosphere. An exact correction would necessitate to acurately evaluate residence time of ^{106}Ru in the atmosphere at each monitoring station which is not easily achievable. Figure 3 shows the same data than figure 2 but corrected for an average ^{106}Ru residence time of 2 days at each observation point. This value of 2 days was inferred from a rough analysis of

[1] http://egasmro.ru/ru/data/overal/refradsit/roshydromet

measurements at points where the sampling period was one day. Although the use of an average correction factor for all observation points has many limitations, figure 3 provides a first attempt to compare ^{106}Ru activities between different points by, at least partially, erasing the bias related to the sampling period. Figure 3 highlights a decreasing gradient of ruthenium concentration from East to West.

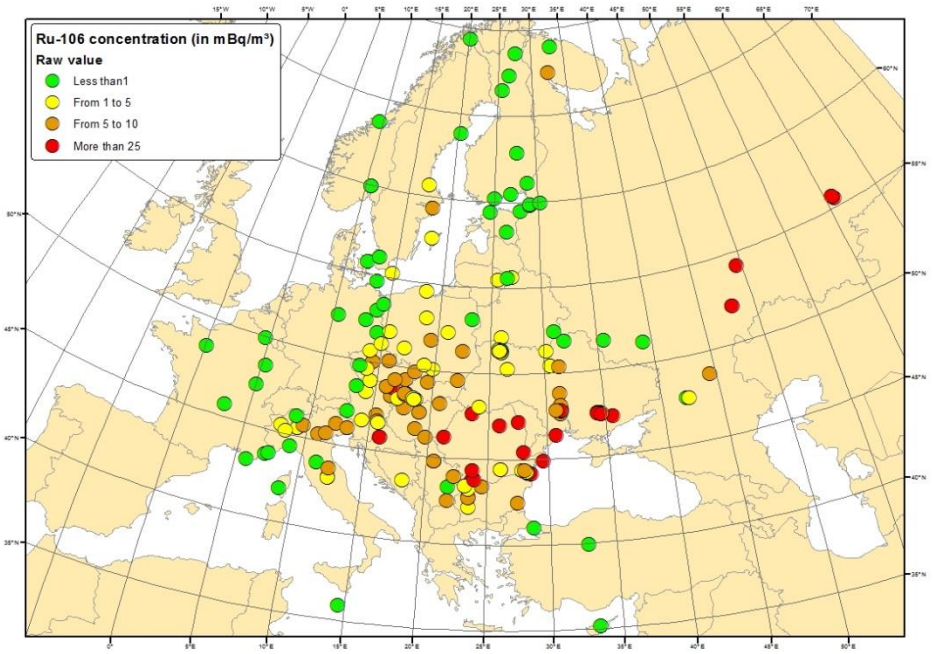

Figure 2 : Average value of the ^{106}Ru concentration in the atmosphere for each monitoring station in Europe/Russia over the whole sampling period during which ruthenium was detected.

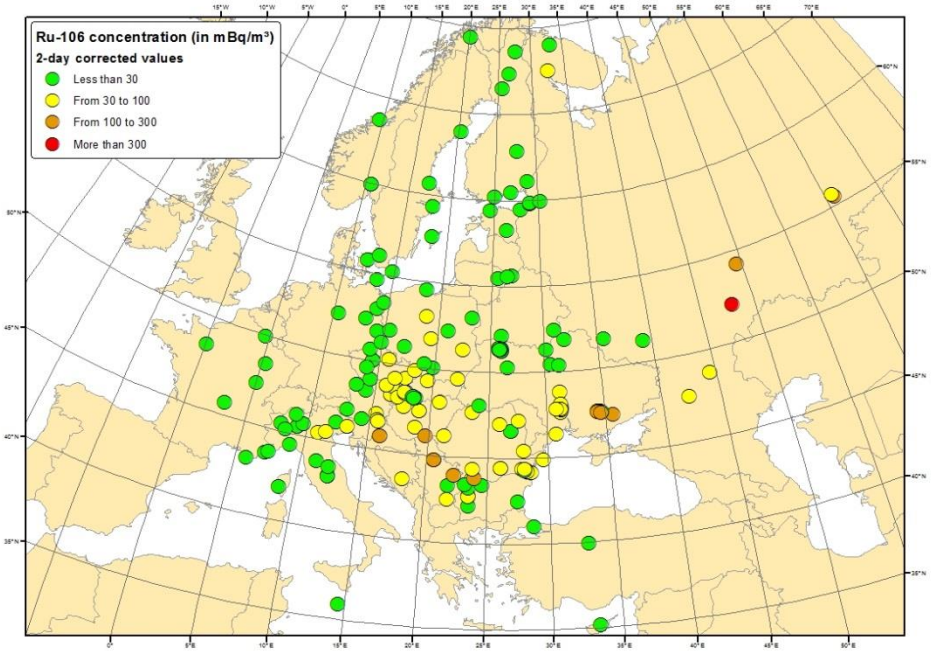

Figure 3 : Similar to figure 2 but data are corrected in order to take into account the fact that, for monitoring stations with sampling periods longer than one day, sampling period exceeds the time during which the ruthenium was present in the atmosphere. See the text for explaination on the correction factor used.

- As far as deposits are considered, the first observations (daily samples) are made in Russia on 23 September at Kyshtym, on 25 September at Argayash and on 26 September at Bugulma, Dema-Doufa, Metlino and Novogornyy (see Table 1)). All of these stations are located in the south of the Urals. These deposits, which can reach several hundred Bq/m^2, are the highest observed on all data analyzed. These levels can be compared to the values of 78 Bq/m^2 observed in Poland between 2 and 4 October in Krakow or in Sweden in Stockholm (20 Bq/m^2 observed between 2 and 4 October).

Location	Latitude	Longitude	Start date	End date	Nuclide	Deposit (Bq/m^2)	Source
Argayash	55,486	60,875	25/09/2017	26/09/2017	Ru-106	115,55	2
Argayash	55,486	60,875	26/09/2017	27/09/2017	Ru-106	109,74	2
Argayash	55,486	60,875	25/09/2017	26/09/2017	Ru-106	15,6	1
Argayash	55,486	60,875	27/09/2017	28/09/2017	Ru-106	7,9	2
Argayash	55,486	60,875	26/09/2017	27/09/2017	Ru-106	112	1
Bugulma	54,536	52,798	26/09/2017	27/09/2017	Ru-106	16	1
Bugulma	54,536	52,798	27/09/2017	28/09/2017	Ru-106	30	1
Dema-Oufa	54,714	55,877	26/09/2017	27/09/2017	Ru-106	17,02	1,2
Metlino	55,789	60,98	26/09/2017	27/09/2017	Ru-106	343,3	2
Metlino	55,789	60,98	26/09/2017	27/09/2017	Ru-106	330	1
Novogornyy	55,633	60,787	26/09/2017	27/09/2017	Ru-106	184,78	1
Novogornyy	55,633	60,787	26/09/2017	27/09/2017	Ru-106	203	1
Novogornyy	55,633	60,787	27/09/2017	28/09/2017	Ru-106	7,9	1
Novogornyy	55,633	60,787	29/09/2017	30/09/2017	Ru-106	28	1
Khudaiberdinski	55,611	60,924	27/09/2017	28/09/2017	Ru-106	9,12	2
Khudaiberdinski	55,611	60,924	27/09/2017	28/09/2017	Ru-106	74	1
Khudaiberdinski	55,611	60,924	29/09/2017	30/09/2017	Ru-106	230,92	2
Khudaiberdinski	55,611	60,924	29/09/2017	30/09/2017	Ru-106	24,7	1
Kyshtym	55,7142	60,8445	23/09/2017	24/09/2017	Ru-106	17,62	2
Morozovsk	48,3441	41,8265	28/09/2017	29/09/2017	Ru-106	17,1	2

Table 1: Values of deposits observed in stations located in Russia. source: Roshydromet internet site :
1) http://egasmro.ru/files/documents/ro_bulletins/byulleten_rorf_09_2017.pdf
2) http://egasmro.ru/files/documents/ro_bulletins/byulleten_rorf_10_2017.pdf

- Finally, as shown in Table 2, at some stations in Sweden, Austria and the Czech Republic, the detection of ^{106}Ru was accompanied by the detection of another isotope of ruthenium, ^{103}Ru (half-life of 39,3 days). The average of the ^{106}Ru/^{103}Ru ratio, on all these observations, is about 4,000. This detection of ^{103}Ru is not systematic for two reasons : 1) this measure requires expertise (in terms of detection level) that not all metrology laboratories have, 2) because of the abovementionned ^{106}Ru/^{103}Ru ratio of about 4,000, it is necessary that the activity of ^{106}Ru is sufficient for ^{103}Ru to be detectable.

Country	station	start date	End date	^{106}Ru mBq/m^3	^{103}Ru mBq/m^3	Ratio (Ru-106/Ru-103)
Austria	Alt Prerau	25/09/2017	02/10/2017	11,1	0,00300	3700
Austria	Straß	25/09/2017	03/10/2017	9,5	0,00300	3167
Austria	Retz	25/09/2017	03/10/2017	12,1	0,00300	4033
Austria	Klagenfurt	25/09/2017	02/10/2017	4,9	0,00200	2450
Austria	Vienna	28/09/2017	04/10/2017	21,7	0,00732	2964
Czech Republic	Praha	26/09/2017	03/10/2017	6,21	0,00062	10016
Czech Republic	Hradec Kralove	26/09/2017	03/10/2017	10,90	0,00257	4241
Czech Republic	Ústí nad Labem	26/09/2017	04/10/2017	4,35	0,00122	3566
Sweden	Stockholm	01/10/2017	02/10/2017	17	0,00470	3617
Sweden	Stockholm	01/10/2017	03/10/2017	14,75	0,00400	3688
Sweden	Stockholm	02/10/2017	03/10/2017	9,8	0,00480	2042
Sweden	Visby	28/09/2017	02/10/2017	5,16	0,00140	3686

Table 2 : Summary of the European air sampling stations where ^{103}Ru was measured. Average value of ^{106}Ru/^{103}Ru ratio is 3930.

In summary, a review of continental European measurements over the period from the end of September to mid-October 2017 leads to the conclusion that (1) the first detections (notably in the form of deposit measurements) took place in the south of the Urals as of 23 September 2017, 2) the observations in the atmosphere (aerosols) in the other countries cover the period from 26 September to mid-October 2017. Finally, the detection of ^{106}Ru was accompanied, at some European stations (Sweden, Czech Republic, Austria), by the detection of ^{103}Ru, the ^{106}Ru /^{103}Ru ratio being about 4,000.

4) Use of a data inversion technique to locate the ^{106}Ru release area

Following this widespread detection of ^{106}Ru in the atmosphere in Europe, IRSN conducted a study to determine the most plausible zone of emission of ^{106}Ru. This study is based on the use of an inverse modeling technique that combines measurements made in the environment (in this case, volume activities in the atmosphere) and atmospheric dispersion modeling. This study assumes that the emission source is located close to the ground.

4.1 Methodology

Numerous approaches have been proposed to identify a point source (Seibert 2000; Issartel et al. 2003; Seibert 2004; Bocquet 2005; Krysta and Bocquet 2007; Krysta and Bocquet; 2008, Kovalets et al. 2011; Tichý et al. 2017) in case of an accidental release in the environment. Bayesian methods (Yee et al. 2008; Dell Monache et al. 2008) draw on a rigorous mathematical formalism but are usually not suitable for an operational use due to

prohibitive computational costs. Other methods consist in the analysis of backward trajectories or retro-plumes (Stohl et al. 1998). The approach used in the present study is inspired by that of Seibert et al. (2000) and is based on inverse modeling techniques where the calculation of the source-receptor matrix is performed in forward mode (as detailed in section 4.2). It aims at identifying the geographical area of a potential release of ^{106}Ru. The approach is divided into four steps as follows :

- The domain area is divided into regular grid cells. Each grid nodes is assumed to be a potential point source.
- For each potential point source, the release rate is assessed by inverse modelling. The method used is described in section 4.2.
- For each potential point source, the agreement between simulated and observed measurements is assessed using several statistical indicators.
- The individual performances of each potential point source are projected by linear interpolation on a map which allows to view the relevance of the potential releases areas.

4.2 Inverse modelling method

The approach used by IRSN allows to estimate the source term using observations in the environment and atmospheric dispersion modelling. Inverse modelling methods, that were intensively developed following the Chernobyl accident, are based on a rigorous mathematical formalism and were proved to be efficient to estimate the source term (Gudiksen et al. 1989; Davoine and Bocquet 2007; Stohl et al. 2012). The method is described in several publications (Winiarek et al. 2011; Winiarek et al. 2012; Saunier et al. 2013; Winiarek et al. 2014; Saunier et al. 2016). It is based on a variationnal approach consisting in the minimization of a cost function $J(\sigma)$ which measures the differences between the model predictions $\mathrm{H}\sigma$ and the real measurements μ. The cost function also includes a background term which adds the differences between a priori emissions σ_b and the updated estimation of the source term σ:

$$J(\sigma) = (\mu - H\sigma)^T R^{-1}(\mu - H\sigma) + (\sigma - \sigma_b)^T B^{-1}(\sigma - \sigma_b)$$

The H source-receptor matrix is the Jacobian matrix computed under the approach proposed by Winiarek et al. (2011). Each column of H represents the dispersion model's response to a unitary release emitted for one radionuclide whose release rate is to be estimated.

$R = E[\varepsilon\varepsilon^T]$ is the error covariance matrix. The vector ε is the observation error aggregating instrumental, representativeness and a fraction of modeling errors. $B = E[(\sigma - \sigma_b)(\sigma - \sigma_b)^T]$ is the background error covariance matrix. Simple parametrization for B and R matrixes are used. It is assumed that they are diagonal and the error variance is the same for all diagonal elements of each matrix (homoscedasticity property):

$$B = m^2 I, \quad m > 0 \text{ and } R = k^2 I, \; k > 0$$

The parameter $\lambda = \frac{k}{m}$ determines the scale of the fluctuations in the source term. When no information is available about the source term, a reasonable choice is to consider σ_b=*0*. Hence the cost function takes the form:

$$J(\sigma) = \|\mu - H\sigma\|^2 + \lambda^2\|\sigma\|^2 \qquad (1)$$

The cost function (1) is directly minimized by using the L-BFGS-B limited-memory quasi-Newton algorithm (Liu and Nocedal, 1989).

4.3 Statistical indicators

For each potential point source, forward simulations of the atmospheric dispersion of ^{106}Ru are performed using the inverted source term. The agreement between simulated and observed air concentrations measurements is assessed using the following statistical indicators:

- The reduction factor of the cost function $J(\sigma)$ per grid cell: since the *a priori* source term σ_b is equal to 0, the initial cost function related to each grid cell contains the same value. Therefore, the factor reduction of the cost function obtained after minimization provides a good indication of the most relevant grid cells as source locations. However, the homoscedasticity property of the parameterization leads to give more weight on the high concentrations values than on the low concentrations values.
- The percent within a factor 2 (fac2) per grid cell: it represents the proportion of the simulated activity concentrations calculated using the inverted source term that is within a factor of 2 of the observed values. The fac2 indicator is complementary to the factor reduction of the cost function since all the concentrations values have the same weight.

4.4 Application to ^{106}Ru source identification

161 air sampling stations have been considered. It leads to 368 ^{106}Ru measurements. Some of these stations did not report ^{106}Ru traces in the atmosphere but are useful to constrain the inverse problem.

The domain used to define the grids of the potential point sources is [-10W, 70E], [34N, 70N] with 2°x 2° spatial resolution. In total, it leads to 720 potential point sources. For each potential point source, daily release rates are estimated by inverse modeling from 24 September to 8 October. Therefore, 720 x 14 atmospheric dispersion simulations have been performed and analyzed. The sensitivity to the parameter λ (see section 4.2) has been tested for a wide range of values [0; 10^7] $\frac{\mu Bq/m^3}{Bq/s}$. Due to a high number of observations used in the inversion, the results obtained are relatively insensitive to the chosen value.

The computation of H matrix is performed using the Eulerian atmospheric dispersion model ldX. This model is part of IRSN's C^{3}X operational platform (Tombette et al., 2014). It is based on the Polair3D chemistry transport model (Boutahar et al., 2004) and has been validated on past nuclear accidents (Quelo et al., 2007). ldX takes into account dry and wet deposition as well as radioactive decay and filiation. Dry deposition is modeled by a simple scheme with a constant deposition velocity: v_{dep} = 2.10^{-3} m/s. For wet scavenging,

the parameterization used is the form $\Lambda_s = \Lambda_0 p_0$, where $\Lambda_0 = 5.10^{-5}$ h/(mm.s) and p_0 the rainfall intensity in millimeters per hour (Baklanov and Sørensen, 2001).
The simulations are performed by forcing ldX with three-hourly operational meteorological data from ARPEGE model provided by Météo France. The spatial resolution of these data is 0.5°x 0.5°. The spatial domain of the ldX simulations is [-10W, 90E], [20N, 70N], which encompasses the total detections. The time resolution is ten minutes and the ldX model provides instantaneous outputs. The spatial resolution is that of the meteorological data (0.5°x 0.5°) and 11 vertical levels between 0 and 4400 m are considered. The release height is taken for the first level of the model, *i.e.* between 0 and 40 m.

4.5 Results

Figure 4 shows a gridded map of the fac2 attached to each potential point source. The higher the fac2, the higher the agreement between modeled and observed air activity concentrations. The fac2 values are higher than 40% in a restricted area located in Russia between Volga and Ural regions. Beyond this geographical area, the fac2 values decrease rapidly down to around 30% at the Russia-Ukraine border. The fac2 values fall below 20% as one goes towards Western Europe and Siberia region. It means that a release from western Europe is an unlikely hypothesis.

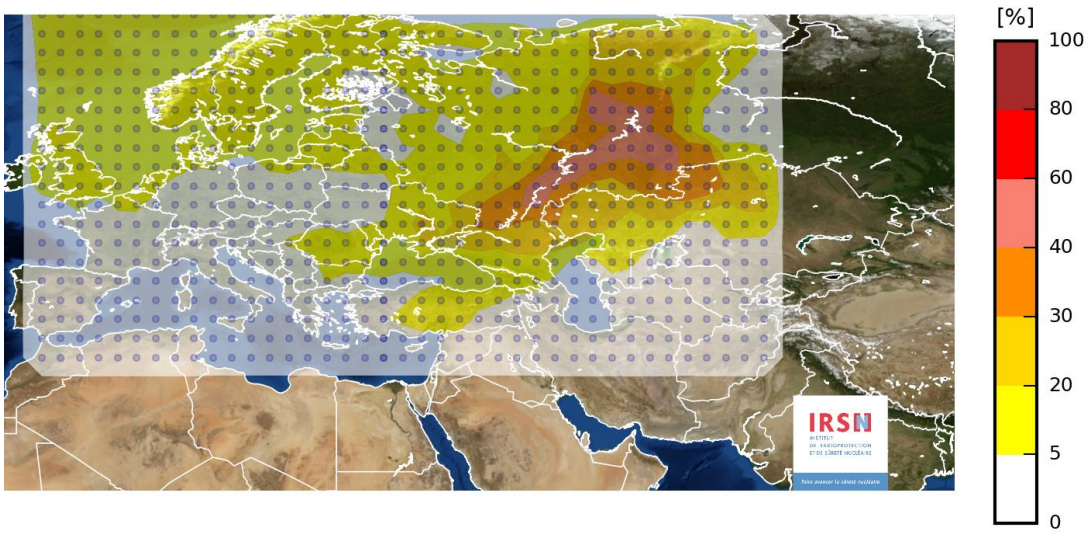

Figure 4: Percent of the simulated activity concentrations that is within a factor of 2 of the observed values. The dots represent the grid of the potential source locations.

Figure 5 represents the reduction factor of the cost function. It confirms the results obtained using the fac2 indicator. Moreover, the calculations performed using this indicator seem to slightly restrict the most reliable area of the potential release between Volga and Ural regions. In this area, the reduction factor is higher than 6 whereas it is lower than 3 close to the Russia-Ukraine border. This result seems not to be consistent with the hypothesis of a point source located in Ukraine.

For the most relevant area of release, the quantity of ^{106}Ru released estimated by inverse modeling ranges from 100 to 300 Tbq. The release would have occurred between 25 September and 28 September. The duration would have not exceeded 24h.

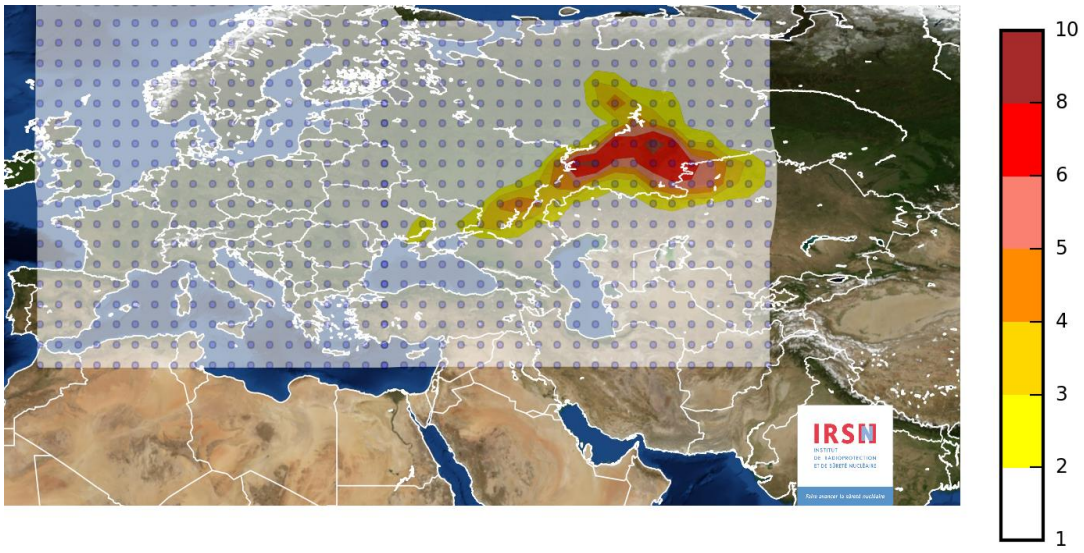

Figure 5 : Reduction factor of the cost function. The dots represent the grid of the potential source locations.

Figure 6 presents the evolution of the atmospheric dispersion as a function of the date when considering a 24 h release of 150 TBq of ^{106}Ru starting on September 25 from a point located in the South Urals region. This pattern of dispersion is very few dependent on the exact location of the source within the most plausible zone of emission (designated by the dot points in figures 4 and 5).

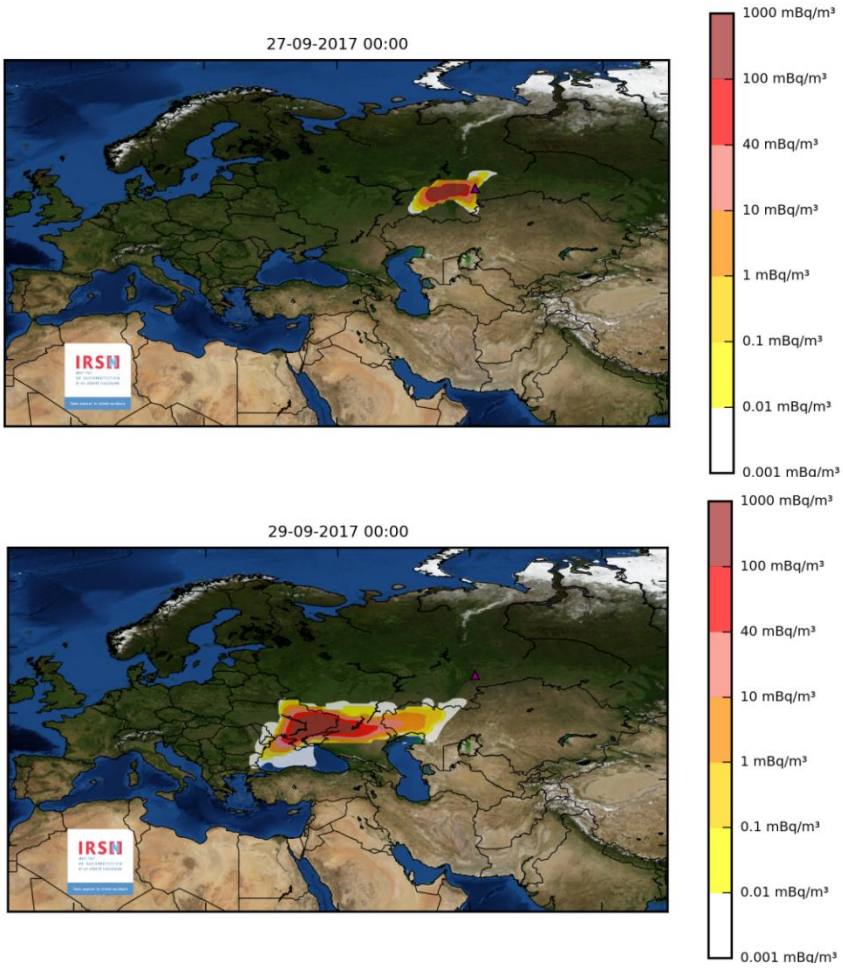

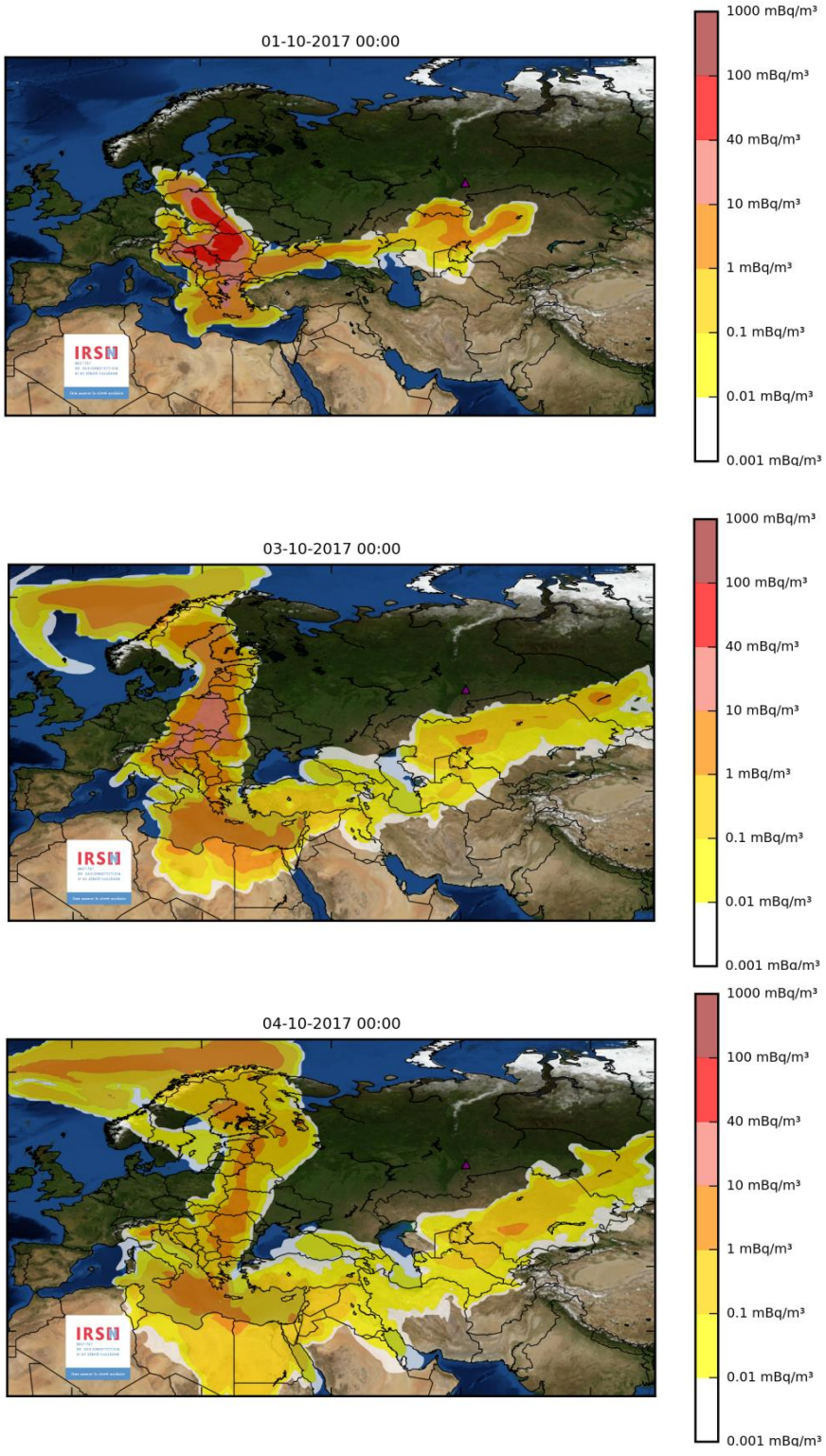

Figure 6 : Evolution of the atmospheric dispersion as a function of the date when considering a 24 h release of 150 TBq of ^{106}Ru starting on September 25 from a point located in the south Ural region.

In summary, following the multiple detections of ^{106}Ru in atmosphere over Europe, inverse modeling methods have been applied in order to identify the areas where a release of ^{106}Ru may have occurred considering a ground level emission. In this study, 720 potential point sources have been considered. The results points out that a release emitted from the regions located between Volga and Ural could best explain the ^{106}Ru detections reported in Europe. A release from other areas seems unlikely. Moreover, for the most relevant area of release, the quantity of ^{106}Ru released estimated by inverse modeling ranges from 100 to 300 TBq. The release would have occurred between 25 September and 28 September. The duration would have not exceeded 24h.

5) Review of the possible origin of ruthenium release

This review takes into account the conclusions of the previous sections (data analysis and simulation results):

- Two artificial radioactive isotopes of ruthenium were detected: ^{106}Ru and, to a lesser extent and in a limited number of monitoring stations (Austria, Czech Republic, Poland and Sweden), ^{103}Ru. No other artificial radionuclide was detected;
- The ratio between the radiological activities of ^{106}Ru and ^{103}Ru (^{106}Ru/^{103}Ru) is of the order of 4,000;
- The released activity of ^{106}Ru is evaluated in the range [100, 300] TBq.

This review is carried out on the basis of information available to IRSN on materials and processes that may lead to ruthenium release. Notably, knowledge of PUREX fuel reprocessing processes is exploited. However, this analysis could be enriched with the analysis of other types of process or specific treatment which are unknown to IRSN.

5.1 Nuclear characteristics and use of ^{106}Ru

The ^{106}Ru and ^{103}Ru half-lives are, respectively, 371,8 days and 39,3 days. The other radioactive isotopes of ruthenium have much shorter half-lives (less than one hour except the isotope 97 with 2.8 days).

^{106}Ru can only be generated as a consequence of a fission reaction. As far as ^{103}Ru is concerned, it can be formed either by fission reaction or as the result of the irradiation of ^{102}Ru. As a consequence, ^{106}Ru can only be produced in irradiated nuclear fuels or in irradiated uranium targets (objects containing a few grams to tens of grams of irradiated enriched uranium (LEU or HEU) for the production of radioactive isotopes).

^{106}Ru is used in the medical field (eye tumor treatment). The sources used in this context have activities of a few MBq to several tens of MBq (IAEA, 2012).

IRSN has no information on any other types of ruthenium source. The use of ^{106}Ru sources for power generation in satellites has also been mentioned. However, IRSN did not find any robust data on this particular use. This point is developed in section 6.

5.2 Interpretation of the data

Release of ruthenium isotopes alone

The detection of ruthenium isotopes alone excludes the possibility of an accidental release from a nuclear reactor which would have resulted in the presence of other radionuclides (iodine, cesium,…). Therefore, the release of ruthenium isotopes alone can only be related to an event involving 1) a ruthenium source, 2) a manufacturing facility for ruthenium sources or 3) an irradiated fuel processing facility (including the particular operations of source manufacturing from the solutions generated in this context).

In the process of irradiated fuels treatment (Purex process), the gaseous fission products (iodine, krypton...) are separated from the other fission products during the shearing of fuels. At this stage of the process, ruthenium is in solid form (metal, RuO_2). However, the chemical form of ruthenium, in normal or accidental operation, changes during the other phases of the process. Thus, depending on the conditions of acidity and temperature, it can be in the following chemical forms:

- Solid form (metal or oxyd RuO_2);
- Liquid form (nitrosyl complex $RuNO(NO_3)_3$);
- Gaseous form (RuO_4).

During the different phases of this process, ruthenium is an element that can pass in gaseous form. In the PUREX process, the production of RuO_4 (gaseous) from Ru nitrosyl, complex is possible if a temperature greater than 100°C is reached. This RuO_4 production increases strongly if the temperature exceeds 120°C.

In the PUREX process, this situation occurs, in normal operation situation, during the vitrification of fission product solutions and it requires special attention (addition of additives, special treatment of the process gases...). However, this can also occur in the case of a loss of cooling of the solution containing fission products. This type of accidental scenario concerns both fuel reprocessing operations and sources production from solutions of fission products (initial solution or solution after used isotopes extraction).

With the exception of operations where the RuO_4 is generated during normal operation (vitrification) and specific measures are taken to treat it, the gaseous effluent treatment systems don't trap the ruthenium in the RuO_4 form. In these systems, the solid radionuclides (cesium, strontium...) are adequately trapped by using high efficiency particulate air filters. However, even if a part of the RuO_4 returns to solid form RuO_2 due to contacts with colder surfaces, the still gaseous fraction will not be trapped by particulate air filters of the ventilation systems and it will be released into the environment (with a rapid transformation into RuO_2 –solid- due to the decrease of temperature). This explains why the only radionuclide released during this type of accidental event is ruthenium (near the facility, the presence of other radioisotopes in the vesicles form, although filtered, cannot be excluded, depending on the efficiency of the particulate air filters).

Such a release occurred, in 2001, in La Hague AREVA nuclear fuel reprocessing plant, due to uncontrolled transfers of gaseous effluents, containing RuO_4, from the vitrification equipment towards the cell containing it. The ^{106}Ru released activity was a few GBq[2].

^{106}Ru released activity

A ^{106}Ru source term ranging from 100 to 300 TBq corresponds to the rejection of a few grams of ^{106}Ru (typically, 1 to 4 grams).

This source term is not compatible with the activity of medical sources (as it is equivalent to several thousands of such sources) and, therefore, an event related to a (or several) ruthenium source(s) can be excluded. This is in agreement with the IAEA report (IAEA, 2017b) that mentionned "*Ru-106 is used in the treatment of ocular cancer. Due to the level of their activities, the brachytherapy sources used in these types of cancer treatment are unlikely to cause, if aerosolized and dispersed, the wide-spread reported air concentrations*".

In a very conservative approach, if we consider the released source term to be equal to that of the material involved in the event and a probability of ^{106}Ru formation by fissioning (uranium 235 fission) of 0.41% (IAEA, 2008), the source term corresponds to the fission of the order of 1 kg of uranium-235. Such mass excludes irradiation targets, which generally contain only a few grams of uranium-235, and the associated processing facility.

Therefore, the only remaining and plausible hypothesis focuses on irradiated fuels processing (including sources produced with these materials).

If one considers the feedback from La Hague AREVA reprocessing plant and the parameters usually considered in the safety analysis (for example for the ruthenium redisposition in the circuits...), the estimated source term corresponds to an event involving a few cubic meters of fission products solution. These volumes are compatible with those involved in fuel reprocessing plants and possibly in the processes associated with the manufacture of radioactive sources fabrication (such as ^{60}Co, ^{137}Cs, ^{90}Sr, ^{144}Ce…). According to available informations, the Mayak radioisotope plant was expected to produce, in 2017, a ^{144}Ce source with an activity ranging from 3,7 to 5,5 PBq (CESOX project). The solution to be used for the manufacture of such a source would have a ^{106}Ru activity reaching several PBq.

^{106}Ru/^{103}Ru ratio

^{106}Ru/^{103}Ru ratio is an indicator of the cooling time of the fuel or the target (time since the end of the irradiation). ^{106}Ru and ^{103}Ru do not appear in the radioactive decay chains of radioactive fission products with periods greater than about one minute. So, after irradiation, their activities vary only because of their radioactive decay. Figure 7 shows calculations of the ^{106}Ru/^{103}Ru ratio as a function of time for a uranium fuel with a variable burn-up rate.

---

2 http://www.gepnucleaire.org/norcot/gepnc/sections/travauxgep/premiere_mission5339/rapport_du_groupe/downloadFile/file/Rapport_ruthenium.pdf?nocache=1280388926.81

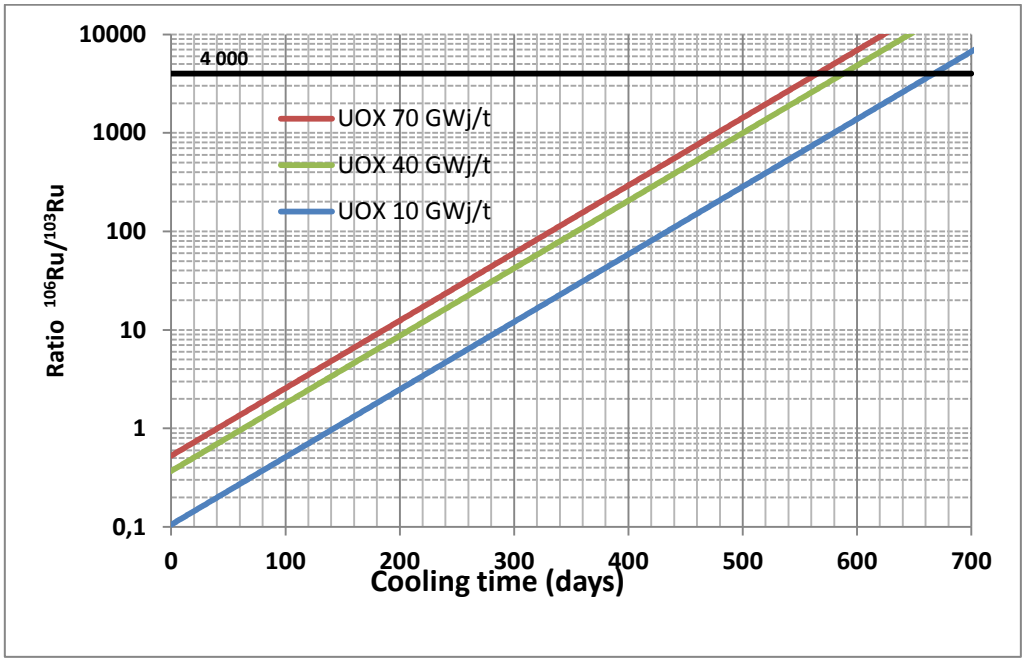

Figure 7 : Evolution with time of the $^{106}Ru/^{103}Ru$ ratio for nuclear fuel with different burn-up.

Based on these calculations, the material involved in the event should have been irradiated a short time ago (of the order of a few years).

It should be noted that, in France, irradiated fuels are treated after 7 to 10 years of cooling time. However, for the production of radioactive sources, the cooling time of the fuels can be much lower. For this type of production, a cooling of a few years appears realistic.

Taking into account the conditions of manufacturing of radioactive sources from solutions of fission products (that require a short cooling time of the fuels, *i.e.* about one or two years), the observation of a $^{106}Ru/^{103}Ru$ ratio around 4,000 allows to exclude an event involving old sources or old fission product solutions. On the other hand, this ratio is potentially compatible with an event involving a source being manufactured, a source newly manufactured, or a recent solution being processed in the objective of manufacturing a source. For example, for the production of the ^{144}Ce source that was to be produced in Mayak in late 2017, spent fuels with two years cooling time were to be used.

5.3 Conclusion

The following table summarizes the consistency between the characteristics of events likely to lead to ^{106}Ru releases and the data gained from measurements and simulations.

Event Type	Data (measurements and simulations)		
	Release of Ruthenium alone	100 to 300 TBq of ^{106}Ru	Presence of ^{103}Ru ^{106}Ru/^{103}Ru = 4,000
Event, concerning a nuclear reactor for example (NPP, research…), involving irradiated fuels or targets (excluding treatment operations of fuels)	Not compatible	(not evaluated)	(not evaluated)
Event concerning operations on targets used in the production of sources, for example in the medical field (activity in MBb)	Compatible	Not compatible	(not evaluated)
Source of ^{106}Ru used in the medical field	Compatible	Not compatible	(not evaluated)
Source of ^{106}Ru used in other fields than the medical one.	Compatible	?	Would concern a very recent source of ^{106}Ru with a very high activity (existence should be confirmed). A release in high altitude is very unlikely (see section 6)
Spent fuel treatment, including production of sources from fission product solutions (based on Ru or other radioisotope as ^{60}Co, ^{90}Sr, ^{137}Cs,…)	Compatible	Compatible	Would concern a short cooling time fuel treatment (source production context, as for the production of the ^{144}Ce CESOX source)
Other events related to irradiated fuel treatments (not known to IRSN)?	?	?	?

From this table, it can be concluded that the most plausible hypothesis to explain the observations (release of ruthenium alone, released activity, ^{103}Ru detection) is related to operations in a spent fuel treatment facility located in South Ural region. The estimated source term (100 to 300 TBq) corresponds to an event involving a few cubic meters of fission products solution. This release could have occurred either during a fuel processing operation or during the production of sources from fission products solutions. The second hypothesis seems plausible as the ^{106}Ru/^{103}Ru ratio (around 4,000) indicates that the fuel treatment operations were conducted on a fuel characterized by a short cooling time (a few years). In particular, the manufacturing of a ^{144}Ce high activity source planned in 2017 at Mayak radioisotope plant should be investigated.

6) Hypothesis of a ruthenium release at high altitude

Following the detection of ruthenium in Europe, the hypothesis of a source of ruthenium at high altitude was evoked through the possibility of the disintegration of a satellite equipped with a Radioisotope Thermoelectric Generator (RTG) fueled with ^{106}Ru. There are several reasons that led IRSN to consider this hypothesis as highly unlikely. These are the following:

- In its various reports dedicated to ruthenium detection (IAEA 2017a, 2017b), IAEA mentioned that "*Some references state that Ru-106 could be used as a source for radioisotope thermoelectric generators (RTG). However such usage is not common due to its short half-life. The IAEA has been in contact with the United Nations Office for Outer Space Affairs (UNOOSA) which has confirmed that no satellite or otherwise re-entries of objects containing Ru-106 RTGs have taken place*". Since then, this has been confirmed by other space agencies, notably Roskosmos, the Russian space agency (Roshydromet, 2017).

- Detection of ^{103}Ru, which is characterized by a very short half-life (39.3 days), is not compatible with the expected satellite life-time.

- if a satellite had burned during its re-entry into the atmosphere it can be stated such a scenario would have impacted the vertical distribution of ^{106}Ru in the air: the higher the altitude, the higher the concentration, as for ^{7}Be, a cosmogenic radionuclide whose production is in the lower stratosphere and upper troposphere. However, it was observed that ^{106}Ru at high-altitude sampling locations was either below detection limit or significantly lower than ^{106}Ru measured at low altitude. In addition, any downdrafts movement from the stratosphere or higher troposphere layers would have led to an increase of the cosmogenic radionuclides such as ^{7}Be or ^{22}Na. During the ^{106}Ru peak detection, both radionuclides remained within their usual range observed at that time of the year which indicates that there was no specific stratosphere-to-troposphere exchange.

- Finally, the re-entry of a satellite into the atmosphere implies that the release would have occurred at high altitude (when the satellite burns). The transfers in the highest layers of the atmosphere are very specific and characterized by a very weak dispersion. Therefore, the transfer of pollutants released at high altitude towards the ground is usually very slow and would be characterized by very small horizontal gradients (which is not the case as it is observed a gradient from Eastern Europe to Western Europe, see figure 3). Moreover, in order to explain the widespread observations, it would be necessary to consider a source-term larger than that considered in the terrestrial release hypothesis which is clearly unrealistic.

As a conclusion and for all the reasons mentioned above, IRSN considers that the hypothesis of a ruthenium source at high altitude generated by the re-entry of a satellite into the atmosphere is very unlikely.

7) General Conclusion

In early October 2017, almost all European countries reported atmospheric detections of radioactive ^{106}Ru, an anthropogenic radionuclide that had never been seen on a continental scale since the Chernobyl accident. In addition to ^{106}Ru, another artificial isotope of ruthenium, ^{103}Ru, was detected in several monitoring stations (Austria, Czech Republic, Poland and Sweden). Analysis of the observed data shows that the first detections took place in the South Ural region. The range of concentrations varied from some tenths $\mu Bq \cdot m^{-3}$ to more than one hundred $mBq \cdot m^{-3}$. The widespread detection at such level

suggested that the source term must have been quite high. Taking into account these observations, IRSN performed further investigations in order to evaluate the source-term, to locate the source of release and to identify the process at the origin of the release.

Inversion techniques, using both observations and meteorological data, were implemented and led to the conclusion that a terrestrial release emitted from the regions located between Volga and Ural could best explain the ^{106}Ru detections reported in Europe. A release from other areas seems unlikely. Moreover, for the most relevant area of release, the quantity of ^{106}Ru released was estimated to range from 100 to 300 TBq. The release would have occurred between 25 September and 28 September. The duration would have not exceeded 24h.

On the basis of information available to IRSN, several hypotheses on the events that could have been at the origin of the release were confronted with both the observations (observation of ruthenium isotopes alone, presence of ^{103}Ru) and the source-term characteristics deduced from the simulations. From this confrontation, it can be concluded that the most plausible hypothesis to explain the observations is related to operations in a spent fuel treatment facility located in a region between Volga and Ural. The estimated source term (100 to 300 TBq) corresponds to an event involving a few cubic-meters of fission products solution. The release could have occurred either during a fuel processing operation or during the production of sources from fission products solution. This last hypothesis seems plausible as the ^{106}Ru/^{103}Ru ratio (around 4,000) indicates that the fuel treatment operations were conducted on a fuel characterized by a short cooling time (a few years). In particular, the manufacturing of a ^{144}Ce high activity source planned in 2017 at Mayak radioisotope plant should be investigated.

References

Baklanov, B. and Sørensen, J.H., 2001: Parameterisation of radionuclides deposition in atmospheric long-range transport modelling. Physics and Chemistry of the Earth, B26, 787-799.

Bocquet, M., 2005: Reconstruction of an atmospheric tracer source using the principle of maximum entropy. II: Applications, Q. J. R. Meteorol. Soc., 131, pp. 2209–2223.

Boutahar, J., Lacour, S., Mallet, V.,Musson-Genon, L., Quelo, D.,Roustan, Y. and Sportisse, B.: 2004 Development and validation of a fully modular platform for the numerical modeling of air pollution: POLAIR. Int. J.Environ. Pollut., 22, 17–28.

Davoine, X. and Bocquet, M., 2007: Inverse modelling-based reconstruction of the Chernobyl source term available for long-range transport. Atmos. Chem. Phys., 7:1549—1564.

Delle Monache, L., Lundquist, J. K., Kosovic, B., Johannesson, G., Dyer, K. M., Aines, R. D.,Chow, F. K., Belles, R. D., Hanley, W. G., Larsen, S. C., Loosmore, G. A., Nitao, J. J., Sugiyama, G. A., Vogt, P. J., 2008: Bayesian inference and Markov chain Monte Carlo sampling to reconstruct a contaminant source on a continental scale. Journal of Applied Meteorology and Climatology 47, 2600–2613. 40, 89, 91.

Gudiksen, P. H., Harvey, T. F., and Lange, R., 1989: Chernobyl Source Term, Atmospheric Dispersion, and Dose Estimation, Health Phys., 57, 697–706.

IAEA, 2008: Handbook of nuclear data for safeguards: database extensions, august 2008. INDC(NDS)-0534, 124p.

IAEA, 2012: Review of seled source designs and manufacturing techniques affecting disused source management, IAEA-TECDOC-1690, 33p.

IAEA, 2017a: International Atomic Energy. Status of Measurements of Ru-106 in Europe. IAEA, Vienna, 2017 – 5p.

IAEA, 2017b: International Atomic Energy. Status of Measurements of Ru-106 in Europe. IAEA, Vienna, 2017 – 19p.

ICRP, 1993: Age-dependent doses to members of the public from intake of radionuclides – Part 2 Ingestion dose coefficient, ICRP publication 67, Ann. ICRP 23 (3-4).
Issartel, J.-P., 2003: Rebuilding sources of linear tracers after atmospheric concentration measurements. Atmos. Chem. Phys., **3,** 2111–2125.
Kovalets I.V., Andronopoulos S., Venetsanos A.G., Bartzis J.G., 2011: Identification of strength and location of stationary point source of atmospheric pollutant in urban conditions using computational fluid dynamics model. Mathematics and Computers in Simulation. - Vol. 82. - P. 244-257.
Krysta, M. and Bocquet, M., 2007: Source reconstruction of an accidental radionuclide release at European scale. Q. J. R. Meteorol. Soc., 133:529—544.
Krysta, M., Bocquet, M., Brandt, J., 2008: Probing ETEX-II data set with inverse modelling. Atmos. Chem. Phys. 8, 3963–3971. 41, 47, 88.
Liu, D.C. and Nocedal, J., 1989: On the limited memory method for large scale optimization, Math. Program. B.,45 (3), 503-528.
Quelo, D., Krysta, M., Bocquet, M., Isnard, O., Minier, Y. and Sportisse, B., 2007: Validation of the Polyphemus platform on the ETEX, Chernobyl and Algeciras cases, Atmospheric Environment, 41, 5300-5315.
Roshydromet, 2017: Report on the source et the possible reasons of the observation of Ru-106 on the territory of the Russian Federation in September-october 2017 (in russian), 137p.
Saunier, O., Mathieu, A., Didier, D., Tombette, M., Quélo, D., Winiarek, V., and Bocquet, M., 2013: An inverse modeling method to assess the source term of the Fukushima Nuclear Power Plant accident using gamma dose rate observations, Atmos. Chem. Phys., 13, 11403–11421, doi:10.5194/acp-13-11403-2013.
Saunier, O., Mathieu, A., Sekiyama, T.T., Kajino, M., Adachi, K., Bocquet, M., Maki, T., Higarashi, Didier, D., 2016: A new perspective on the Fukushima releases brought by newly available ^{137}Cs air concentration observations and reliable meteorological fields. Presented at the 17th International Conference on Harmonisation within Atmospheric Dispersion Modelling for Regulatory Purposes, Budapest, Hungary.
Seibert, P., 2000: Methods for source determination in the context of the CTBT radionuclide monitoring system. Proceedings Informal Workshop on Meteorological Modelling in Support of CTBT Verification (Vienna, December 2000)
Seibert, P., 2000: Inverse modelling of sulfur emissions in Europe based on trajectories, In: Inverse Methods in Global Biogeochemical Cycles, edited by: Kasibhatla, P., Heimann, M., Rayner, P., Mahowald, N., Prinn, R. G., and Hartley, D. E., 147–154, Geophysical Monograph 114, American Geophysical Union, ISBN 0-87590-097-6, Washington, DC, USA.
Seibert, P., and Frank A., 2004: Source-receptor matrix calculation with a Lagrangian particle dispersion model in backward mode. Atmospheric Chemistry & Physics, 4 :51-63.
Stohl, A., 1998: Computation, accuracy and applications of trajectories – a review and bibliography. Atmos. Environ. 32, 947–966.
Stohl, A., Seibert, P., Wotawa, G., Arnold, D., Burkhart, J.F., Eckhardt, S., Tapia, C., Vargas, A. and Yasunari, T.J., 2012: Xenon-133 and caesium-137 releases into the atmosphere from the Fukushima Dai-ichi nuclear power plant: determination of the ST, atmospheric dispersion, and deposition, Atmos. Chem. Phys., 12, 2313-2343.
Tichý, O., Šmídl, V., Hofman, R., Šindelářová, K., Hýža, M., and Stohl, A., 2017: Bayesian inverse modeling and source location of an unintended I-131 release in Europe in the fall of 2011, Atmos. Chem. Phys. Discuss., doi:10.5194/acp-2017-206, in review.
Tombette, M., Quentric, E., Quélo, D., Benoit, J.-p., Mathieu, A., Korsakissok, I. and Didier, D., 2014: C3X : A software platform for assessing the consequences of an accidental release of radioactivity into the atmosphere. International Radiation Protection Association congress, Geneva.
Winiarek, V., Vira, J., Bocquet, M., Sofiev, M. and Saunier, O., 2011: Towards the operational estimation of a radiological plume using data assimilation after a radiological accidental atmospheric release, Atmos. Env., 45, 2944-2955.
Winiarek V., Bocquet M., Saunier O. and Mathieu A., 2012: Estimation of errors in the inverse modeling of accidental release of atmospheric pollutant: Application to the reconstruction of the cesium-137 and iodine-131 STs from the Fukushima Daiichi power plant. J. Geophys. Res., 117, D05122.
Winiarek, V., Bocquet, M., Duhanyan, N., Roustan, Y., Saunier, O., and Mathieu, A., 2014: Estimation of the caesium-137 source term from the Fukushima Daiichi nuclear power plant

using a consistent joint assimilation of air concentration and deposition observations, Atmos. Environ., 82, 268–279.
Yee, E., Lien, F.-S., Keats, A., and D'Amours, R., 2008: Bayesian inversion of concentration data: source reconstruction in the adjoint representation of atmospheric diffusion, Journal of Wind Engineering and Industrial Aerodynamics, vol. 96, no. 10-11, pp. 1805–1816.

ANNEXE 1

Location	Measured Value (mBq/m^3)	Latitude	Longitude	Start Sampling [UTC]	End Sampling [UTC]
Ajaccio	0.0082	41.91826	8.79281	02/10/2017 08:30	09/10/2017 10:30
Allinge	1.8	55.27	14.8	30/09/2017 00:00	07/10/2017 00:00
Alt-Prerau	11,000	48.79644	16.475253	25/09/2017 00:00	02/10/2017 00:00
Angermünde	0.16	53.03145	13.99079	25/09/2017 00:00	02/10/2017 00:00
Ankara	0.018	39.92077	32.85411	04/10/2017 00:00	10/10/2017 00:00
Ankara	< 0.006	39.92077	32.85411	10/10/2017 00:00	13/10/2017 00:00
Arad	< MDA	46.191	21.326	28/09/2017 03:00	28/09/2017 14:00
Arad	< MDA	46.191	21.326	29/09/2017 03:00	29/09/2017 14:00
Arad	< MDA	46.191	21.326	30/09/2017 03:00	30/09/2017 14:00
Arad	64,42	46.191	21.326	01/10/2017 03:00	01/10/2017 14:00
Arad	30,41	46.191	21.326	02/10/2017 03:00	02/10/2017 14:00
Arad	9,31	46.191	21.326	03/10/2017 03:00	03/10/2017 14:00
Arad	< MDA	46.191	21.326	04/10/2017 03:00	04/10/2017 14:00
Arad	<MDA	46.1866	21.3123	28/09/2017 00:00	28/09/2017 00:00
Arad	<MDA	46.1866	21.3123	29/09/2017 00:00	29/09/2017 00:00
Arad	<MDA	46.1866	21.3123	30/09/2017 00:00	30/09/2017 00:00
Arad	64.42	46.1866	21.3123	01/10/2017 00:00	01/10/2017 00:00
Arad	30.41	46.1866	21.3123	02/10/2017 00:00	02/10/2017 00:00
Arad	<MDA	46.1866	21.3123	03/10/2017 00:00	03/10/2017 00:00
Argayash	41,6	55.486	60.875	26/09/2017 00:00	01/10/2017 00:00
Arkhangelsk	<LD	64.552077	40.520266	25/09/2017 00:00	06/10/2017 00:00
Arkona	0.0142	54.67812	13.43355	25/09/2017 00:00	02/10/2017 00:00
Athens	4.07	37.9838	23.7275	27/09/2017 00:00	03/10/2017 00:00
Athens	2.24	37.9838	23.7275	03/10/2017 00:00	04/10/2017 00:00
Athens	0.79	37.9838	23.7275	04/10/2017 00:00	06/10/2017 00:00
Athens	0.2	37.9838	23.7275	05/10/2017 00:00	10/10/2017 00:00
Baia Mare	< MDA	47.654	23.589	28/09/2017 03:00	28/09/2017 14:00
Baia Mare	< MDA	47.654	23.589	29/09/2017 03:00	29/09/2017 14:00
Baia Mare	< MDA	47.654	23.589	30/09/2017 03:00	30/09/2017 14:00
Baia Mare	47,467	47.654	23.589	01/10/2017 03:00	01/10/2017 14:00
Baia Mare	38,212	47.654	23.589	02/10/2017 03:00	02/10/2017 14:00
Baia Mare	24,6	47.654	23.589	03/10/2017 03:00	03/10/2017 14:00
Baia Mare	< MDA	47.654	23.589	04/10/2017 03:00	04/10/2017 14:00
Baia Mare	-	47.6567	23.585	28/09/2017 00:00	28/09/2017 00:00
Baia Mare	<MDA	47.6567	23.585	29/09/2017 00:00	29/09/2017 00:00
Baia Mare	<MDA	47.6567	23.585	30/09/2017 00:00	30/09/2017 00:00
Baia Mare	47.47	47.6567	23.585	01/10/2017 00:00	01/10/2017 00:00
Baia Mare	38.12	47.6567	23.585	02/10/2017 00:00	02/10/2017 00:00
Baia Mare	24.6	47.6567	23.585	03/10/2017 00:00	03/10/2017 00:00
Balakovo NPP	33,2	52.088	47.983	01/09/2017 00:00	02/10/2017 00:00
Balakovo NPP	63,6	52.088	47.983	02/10/2017 00:00	02/11/2017 00:00
Baryshevka (Kyiv region)	14.9	50.3507	31.3189	28/09/2017 00:00	30/09/2017 00:00
Baryshevka (Kyiv region)	13.9	50.3507	31.3189	29/09/2017 00:00	03/10/2017 00:00

Location	Measured Value (mBq/m)	Latitude	Longitude	Start Sampling [UTC]	End Sampling [UTC]
Bechet	< MDA	43.782	23.95	28/09/2017 03:00	29/09/2017 02:00
Bechet	66,6	43.782	23.95	29/09/2017 03:00	30/09/2017 02:00
Bechet	127,57	43.782	23.95	30/09/2017 03:00	01/10/2017 02:00
Bechet	18,1	43.782	23.95	01/10/2017 03:00	02/10/2017 02:00
Bechet	< MDA	43.782	23.95	02/10/2017 03:00	03/10/2017 02:00
Bechet	< MDA	43.782	23.95	03/10/2017 03:00	04/10/2017 02:00
Bechet	< MDA	43.782	23.95	04/10/2017 03:00	05/10/2017 02:00
Bechet	<MDA	43.7843	23.9597	28/09/2017 00:00	28/09/2017 00:00
Bechet	66.6	43.7843	23.9597	29/09/2017 00:00	29/09/2017 00:00
Bechet	127.59	43.7843	23.9597	30/09/2017 00:00	30/09/2017 00:00
Bechet	18.1	43.7843	23.9597	01/10/2017 00:00	01/10/2017 00:00
Bechet	<MDA	43.7843	23.9597	02/10/2017 00:00	02/10/2017 00:00
Bechet	<MDA	43.7843	23.9597	03/10/2017 00:00	03/10/2017 00:00
Belgrad	40,000	44.766799	20.6	02/10/2017 10:00	02/10/2017 10:00
Belgrad	18,000	44.766799	20.6	03/10/2017 10:00	03/10/2017 10:00
Belgrad	<MDA	44.766799	20.6	05/10/2017 10:00	05/10/2017 10:00
Belluno	2.62	46.165278	12.246111	29/09/2017 00:00	02/10/2017 00:00
Belluno	18.6	46.165278	12.246111	02/10/2017 00:00	03/10/2017 00:00
Belluno	2.17	46.134444	12.221667	05/10/2017 00:00	06/10/2017 00:00
Beloyarsk NPP	<0,0035	56.84178	61.31922	18/09/2017 00:00	25/09/2017 00:00
Beloyarsk NPP	<0,0035	56.84178	61.31922	02/10/2017 00:00	09/10/2017 00:00
Bergamo	3.8	45.686667	9.679444	29/09/2017 00:00	02/10/2017 00:00
Bergamo	2.5	45.686667	9.679444	29/09/2017 00:00	02/10/2017 00:00
Bergamo	12.2	45.686667	9.679444	02/10/2017 00:00	03/10/2017 00:00
Bergamo	6.9	45.686667	9.679444	03/10/2017 00:00	03/10/2017 00:00
Białystok	0.23	53.1325	23.1688	25/09/2017 00:00	02/10/2017 00:00
Bilibino NPP	<0,066	68.05135	166.54008	09/10/2017 00:00	12/10/2017 00:00
Bilthoven	< 4.3E-03	52.1365	5.2104	21/09/2017 00:00	28/09/2017 00:00
Bilthoven	< 7.6E-03	52.1365	5.2104	28/09/2017 00:00	03/10/2017 00:00
Bilthoven	< 21.5E-03	52.1365	5.2104	05/10/2017 00:00	06/10/2017 00:00
Bolshaya Murta	0,0785	56.909	93.120586	04/10/2017 00:00	05/10/2017 00:00
Bolshaya Murta	0,1128	56.909	93.120586	06/10/2017 00:00	07/10/2017 00:00
Braslaw	2.7	55.633333	27.033333	03/10/2017 00:00	04/10/2017 00:00
Bratislava	15,000	48.1486	17.1077	29/09/2017 00:00	29/09/2017 00:00
Bratislava	9.8	48.1486	17.1077	27/09/2017 00:00	03/10/2017 00:00
Bregenz	< 1.7E-02	47.504849	9.726419	26/09/2017 06:40	03/10/2017 09:00
Brno	21.1	49.2	16.6	26/09/2017 09:00	03/10/2017 09:00
București	< MDA	44.431	26.122	28/09/2017 03:00	28/09/2017 14:00
București	< MDA	44.431	26.122	29/09/2017 03:00	29/09/2017 14:00
București	145	44.431	26.122	30/09/2017 03:00	30/09/2017 14:00
București	18,096	44.431	26.122	01/10/2017 03:00	01/10/2017 14:00
București	< MDA	44.431	26.122	02/10/2017 03:00	02/10/2017 14:00
București	< MDA	44.431	26.122	03/10/2017 03:00	03/10/2017 14:00
București	< MDA	44.431	26.122	04/10/2017 03:00	04/10/2017 14:00
Bucureşti	<MDA	44.393	26.1471	28/09/2017 00:00	28/09/2017 00:00

Location	Measured Value (mBq/m^3)	Latitude	Longitude	Start Sampling [UTC]	End Sampling [UTC]
Bucureşti	37.9	44.393	26.1471	29/09/2017 00:00	29/09/2017 00:00
Bucureşti	145,000	44.393	26.1471	30/09/2017 00:00	30/09/2017 00:00
Bucureşti	18.1	44.393	26.1471	01/10/2017 00:00	01/10/2017 00:00
Bucureşti	<MDA	44.393	26.1471	02/10/2017 00:00	02/10/2017 00:00
Bucureşti	<MDA	44.393	26.1471	03/10/2017 00:00	03/10/2017 00:00
Budapest	0.47	47.2952	19.0223	22/09/2017 00:00	25/09/2017 00:00
Budapest	2.74	47.2952	19.0223	25/09/2017 00:00	26/09/2017 00:00
Budapest	1.72	47.2952	19.0223	26/09/2017 00:00	27/09/2017 00:00
Budapest	1.99	47.2952	19.0223	27/09/2017 00:00	28/09/2017 00:00
Budapest	12,000	47.2952	19.0223	25/09/2017 00:00	02/10/2017 00:00
Budapest	10.6	47.2952	19.0223	25/09/2017 00:00	02/10/2017 00:00
Budapest	14.7	47.2952	19.0223	25/09/2017 00:00	02/10/2017 00:00
Budapest	1.94	47.2952	19.0223	28/09/2017 00:00	29/09/2017 00:00
Budapest	33.8	47.2952	19.0223	29/09/2017 00:00	02/10/2017 00:00
Budapest	27.6	47.2952	19.0223	02/10/2017 00:00	03/10/2017 00:00
Budapest	9.9	47.2952	19.0223	03/10/2017 00:00	04/10/2017 00:00
Caceres	<MDA	39.48	-6.34	05/10/2017 07:00	
Cernavodă	81,276	44.349	28.049	29/09/2017 03:00	30/09/2017 02:00
Cernavodă	47,233	44.317696	28.052258	30/09/2017 03:00	01/10/2017 02:00
Cernavodă	< MDA	44.349	28.049	01/10/2017 03:00	02/10/2017 02:00
Cernavodă	< MDA	44.349	28.049	02/10/2017 03:00	03/10/2017 02:00
Cernavodă	< MDA	44.349	28.049	03/10/2017 03:00	04/10/2017 02:00
Cernavodă	< MDA	44.349	28.049	04/10/2017 03:00	05/10/2017 02:00
Cernavodă	< MDA	44.349	28.049	05/10/2017 03:00	06/10/2017 02:00
Cernavodă	<MDA	44.3276	28.0306	28/09/2017 00:00	28/09/2017 00:00
Cernavodă	81.28	44.3276	28.0306	29/09/2017 00:00	29/09/2017 00:00
Cernavodă	57.88	44.3276	28.0306	30/09/2017 00:00	30/09/2017 00:00
Cernavodă	<MDA	44.3276	28.0306	01/10/2017 00:00	01/10/2017 00:00
Cernavodă	<MDA	44.3276	28.0306	02/10/2017 00:00	02/10/2017 00:00
Cernavodă	<MDA	44.3276	28.0306	03/10/2017 00:00	03/10/2017 00:00
Červený Hrádok	4.89	48.2999	18.3833	22/09/2017 00:00	04/10/2017 00:00
České Budějovice	1.9	48.967	14.467	26/09/2017 07:00	03/10/2017 07:00
Chernobyl	2.5	51.2763	30.2219	29/09/2017 00:00	01/10/2017 12:00
Chernobyl	2.5	51.2763	30.2219	29/09/2017 00:00	03/10/2017 00:00
Chilton	<3.4E-02	51.5747	-1.3191	02/10/2017 12:00	09/10/2017 10:40
Constanța	< MDA	44.173	28.635	28/09/2017 03:00	29/09/2017 02:00
Constanța	88,1	44.173	28.635	29/09/2017 03:00	30/09/2017 02:00
Constanța	44,31	44.173	28.635	30/09/2017 03:00	01/10/2017 02:00
Constanța	< MDA	44.173	28.635	01/10/2017 03:00	02/10/2017 02:00
Constanța	< MDA	44.173	28.635	02/10/2017 03:00	03/10/2017 02:00
Constanța	< MDA	44.173	28.635	03/10/2017 03:00	04/10/2017 02:00
Constanța	< MDA	44.173	28.635	04/10/2017 03:00	05/10/2017 02:00
Constanţa	<MDA	44.1598	28.6348	28/09/2017 00:00	28/09/2017 00:00
Constanţa	88.1	44.1598	28.6348	29/09/2017 00:00	29/09/2017 00:00
Constanţa	44.31	44.1598	28.6348	30/09/2017 00:00	30/09/2017 00:00

Location	Measured Value (mBq/m^3)	Latitude	Longitude	Start Sampling [UTC]	End Sampling [UTC]
Constanţa	<MDA	44.1598	28.6348	01/10/2017 00:00	01/10/2017 00:00
Constanţa	<MDA	44.1598	28.6348	02/10/2017 00:00	02/10/2017 00:00
Constanţa	<MDA	44.1598	28.6348	03/10/2017 00:00	03/10/2017 00:00
Cottbus	0.678	51.77614	14.31669	25/09/2017 00:00	02/10/2017 00:00
Craiova	< MDA	44.325	23.814	28/09/2017 03:00	29/09/2017 02:00
Craiova	59,81	44.325	23.814	29/09/2017 03:00	30/09/2017 02:00
Craiova	106,27	44.325	23.814	30/09/2017 03:00	01/10/2017 02:00
Craiova	33,12	44.325	23.814	01/10/2017 03:00	02/10/2017 02:00
Craiova	< MDA	44.325	23.814	02/10/2017 03:00	03/10/2017 02:00
Craiova	< MDA	44.325	23.814	03/10/2017 03:00	04/10/2017 02:00
Craiova	< MDA	44.325	23.814	04/10/2017 03:00	05/10/2017 02:00
Craiova	<MDA	44.3302	23.7949	28/09/2017 00:00	28/09/2017 00:00
Craiova	59.81	44.3302	23.7949	29/09/2017 00:00	29/09/2017 00:00
Craiova	106.27	44.3302	23.7949	30/09/2017 00:00	30/09/2017 00:00
Craiova	23.8	44.3302	23.7949	01/10/2017 00:00	01/10/2017 00:00
Craiova	<MDA	44.3302	23.7949	02/10/2017 00:00	02/10/2017 00:00
Craiova	<MDA	44.3302	23.7949	03/10/2017 00:00	03/10/2017 00:00
Dimitrovgrad	35	54.2106	49.5717	22/09/2017 00:00	29/09/2017 00:00
Dolgoprudny	<LD	54.947	37.499	29/09/2017 00:00	06/10/2017 00:00
Ekaterinburg	<LD	56.837	60.605	26/09/2017 00:00	05/10/2017 00:00
Fetesti	3.18	44.3833	27.8333	06/09/2017 00:00	06/10/2017 00:00
Firenze	0.5	43.777222	11.248611	30/09/2017 00:00	02/10/2017 00:00
Firenze	1.4	43.777222	11.248611	02/10/2017 00:00	03/10/2017 00:00
Firenze	< 0.3	43.777778	11.249167	04/10/2017 00:00	05/10/2017 00:00
Fürstenzell	0.0195	48.54421	13.35245	25/09/2017 00:00	02/10/2017 00:00
Gävle	< 0.01	60.67	17.19	26/09/2017 10:10	29/09/2017 11:45
Gävle	3.78	60.67	17.19	29/09/2017 11:45	03/10/2017 05:00
Gävle	< 0.12	60.67	17.19	03/10/2017 05:00	06/10/2017 08:00
GDYNIA	3.62	54.5189	18.5305	25/09/2017 00:00	02/10/2017 00:00
GENOVA	0.5	44.2535	8.5454	29/09/2017 00:00	02/10/2017 00:00
Gherghina	3.39	44.3226	28.1819	05/09/2017 00:00	05/10/2017 00:00
Görlitz	4.91	51.16234	14.95027	25/09/2017 00:00	02/10/2017 00:00
Görlitz	4.57	51.16234	14.95027	02/10/2017 00:00	04/10/2017 00:00
Graz	9,000	47.075488	15.450536	25/09/2017 11:53	02/10/2017 08:20
Graz	36,000	47.075488	15.450536	02/10/2017 08:25	03/10/2017 10:16
Graz	1,000	47.075488	15.450536	04/10/2017 08:00	05/10/2017 07:00
Graz	1,000	47.075488	15.450536	05/10/2017 07:05	06/10/2017 07:15
Greifswald	0.00896	54.09619	13.40509	25/09/2017 00:00	02/10/2017 00:00
Győr	14.3	47.6875	17.6504	26/09/2017 00:00	03/10/2017 00:00
Haderslev	<MDA	55.23	9.5	27/09/2017 00:00	04/10/2017 00:00
Harku	<MDA	59.3863	24.5788	24/09/2017 00:00	01/10/2017 00:00
Helsinki	0.077	60.1699	24.9384	28/09/2017 00:00	03/10/2017 00:00
Helsinki	0.849	60.1699	24.9384	03/10/2017 00:00	04/10/2017 00:00
Helsinki	<MDA	60.1699	24.9384	05/10/2017 00:00	06/10/2017 00:00

Location	Measured Value (mBq/m^3)	Latitude	Longitude	Start Sampling [UTC]	End Sampling [UTC]
Holešov	7.9	49.317	15.67	25/09/2017 07:20	02/10/2017 07:20
Hradec Králové	24.9	50.233	15.87	26/09/2017 08:25	03/10/2017 06:47
Hradec Králové	4.19	50.233	15.87	03/10/2017 06:50	03/10/2017 13:50
Hradec Králové	< 0.3	50.233	15.87	04/10/2017 13:40	05/10/2017 13:40
Iași	< MDA	47.181	27.583	28/09/2017 03:00	29/09/2017 02:00
Iași	80,75	47.181	27.583	29/09/2017 03:00	30/09/2017 02:00
Iași	65,797	47.181	27.583	30/09/2017 03:00	01/10/2017 02:00
Iași	< MDA	47.181	27.583	01/10/2017 03:00	02/10/2017 02:00
Iași	< MDA	47.181	27.583	02/10/2017 03:00	02/10/2017 02:00
Iași	< MDA	47.181	27.583	03/10/2017 03:00	03/10/2017 02:00
Iași	< MDA	47.181	27.583	04/10/2017 03:00	05/10/2017 02:00
Iaşi	<MDA	47.1585	27.6014	28/09/2017 00:00	28/09/2017 00:00
Iaşi	<MDA	47.1585	27.6014	29/09/2017 00:00	29/09/2017 00:00
Iaşi	<MDA	47.1585	27.6014	30/09/2017 00:00	30/09/2017 00:00
Iaşi	<MDA	47.1585	27.6014	01/10/2017 00:00	01/10/2017 00:00
Iaşi	<MDA	47.1585	27.6014	02/10/2017 00:00	02/10/2017 00:00
Iaşi	<MDA	47.1585	27.6014	03/10/2017 00:00	03/10/2017 00:00
Innsbruck	< 1.4E-02	47.259963	11.356563	25/09/2017 07:15	02/10/2017 06:55
Innsbruck	< 0.3	47.259963	11.356563	02/10/2017 07:03	04/10/2017 06:29
Innsbruck	< 1	47.259963	11.356563	04/10/2017 06:30	05/10/2017 07:22
Innsbruck	<MDA	47.259963	11.356563	05/10/2017 07:27	06/10/2017 07:15
Istanbul	0.0177	41.00527	28.97696	13/09/2017 00:00	06/10/2017 00:00
Istanbul	0.3296	41.00527	28.97696	06/10/2017 00:00	10/10/2017 00:00
Istanbul	< 0.041	41.00527	28.97696	10/10/2017 00:00	13/10/2017 00:00
Ivalo	0.156	68.6576	27.5397	02/10/2017 00:00	05/10/2017 00:00
IVREA	0.88	45.474167	7.874167	27/09/2017 00:00	03/10/2017 00:00
IVREA	1.17	45.474167	7.874167	05/10/2017 00:00	06/10/2017 00:00
Jaslovské Bohunice 1	10.3	48.4761	17.65	29/09/2017 00:00	06/10/2017 00:00
Jaslovské Bohunice 2	9.46	48.4761	17.65	29/09/2017 00:00	06/10/2017 00:00
Jaslovské Bohunice 3	10.74	48.4761	17.65	27/09/2017 00:00	04/10/2017 00:00
Jeleznogorsk	0,02	56.251984	93.532364	01/10/2017 00:00	31/10/2017 00:00
Kalinin NPP	<0,0014	57.9043	35.0905	19/09/2017 00:00	03/10/2017 00:00
Kátlovce	9.83	48.5221	17.6059	27/09/2017 00:00	04/10/2017 00:00
Katowice	0.6	50.2649	19.0238	25/09/2017 00:00	02/10/2017 00:00
Khmelnitsky NPP	1.4	50.3025	26.6522	29/09/2017 00:00	03/10/2017 00:00
Kiev	2.2	50.4501	30.5234	28/09/2017 00:00	30/09/2017 00:00
Kiruna	< 0.003	67.84	20.42	25/09/2017 10:40	02/10/2017 05:02
Klagenfurt	4.8	46.648407	14.318416	25/09/2017 10:02	02/10/2017 08:18
Kola NPP	19	67.46528	32.48111	28/09/2017 00:00	05/10/2017 00:00
Kraków	1.67	50.0647	19.945	25/09/2017 00:00	02/10/2017 00:00
Krusk NPP	0,23	51.675104	35.6042	01/09/2017 00:00	30/09/2017 00:00
Krusk NPP	0,084	51.675104	35.6042	01/10/2017 00:00	31/10/2017 00:00

Location	Measured Value (mBq/m^3)	Latitude	Longitude	Start Sampling [UTC]	End Sampling [UTC]
Kuopiossa	0.219	62.898	27.6782	02/10/2017 00:00	05/10/2017 00:00
Kurchatov city	<LD	51.665182	35.648679	29/09/2017 00:00	04/10/2017 00:00
Kyiv	2.2	50.4501	30.5234	29/09/2017 00:00	03/10/2017 00:00
La Seyne sur Mer	0.0074	43.10675	5.8847	26/09/2017 08:25	03/10/2017 11:30
La Seyne sur Mer	0.0197	43.10675	5.8847	26/09/2017 08:25	03/10/2017 11:30
La Seyne sur Mer	0.00155	43.10675	5.8847	26/09/2017 08:25	03/10/2017 11:30
La Seyne sur Mer	0.00103	43.10675	5.8847	26/09/2017 08:25	03/10/2017 11:30
Laa a/d Thaya	< 4.6	48.7317	16.3917	28/09/2017 17:45	29/09/2017 18:46
Laa a/d Thaya	< 4.5	48.7317	16.3917	29/09/2017 18:46	30/09/2017 19:50
Laa a/d Thaya	38,000	48.7317	16.3917	30/09/2017 19:50	01/10/2017 20:52
Laa a/d Thaya	40,000	48.7317	16.3917	01/10/2017 20:52	02/10/2017 10:13
Laa a/d Thaya	23,000	48.7317	16.3917	02/10/2017 18:45	03/10/2017 09:32
Leningrad NPP	0,073	59.83071	29.057	25/09/2017 00:00	06/10/2017 00:00
Leningrad NPP	<0,005	59.83071	29.057	01/10/2017 00:00	31/10/2017 00:00
Leningrad NPP	0,14	59.869669	29.081386	29/09/2017 00:00	31/10/2017 00:00
Leopoldschlag	< 4.9	48.6182	14.5018	28/09/2017 12:13	29/09/2017 12:31
Leopoldschlag	< 4.6	48.6182	14.5018	29/09/2017 12:31	30/09/2017 12:49
Leopoldschlag	< 4.5	48.6182	14.5018	30/09/2017 12:49	01/10/2017 13:07
Leopoldschlag	< 4.2	48.6182	14.5018	01/10/2017 13:07	02/10/2017 16:25
Levice	3.67	48.2164	18.6004	20/09/2017 00:00	04/10/2017 00:00
Linz	0.7	48.267505	14.280038	25/09/2017 09:50	02/10/2017 09:52
Linz	8,000	48.267505	14.280038	02/10/2017 10:00	03/10/2017 10:25
Linz	< 0.2	48.267505	14.280038	04/10/2017 09:35	05/10/2017 09:30
Linz	< 0.1	48.267505	14.280038	05/10/2017 09:33	06/10/2017 09:36
Ljubljana	3.1	46.0558	14.5083	04/09/2017 10:00	02/10/2017 00:00
Ljubljana	37,000	46.0558	14.5083	02/10/2017 10:00	04/10/2017 10:00
Ljubljana	4,000	46.0558	14.5083	04/10/2017 10:00	05/10/2017 10:00
Ljungbyhed	< 0.004	56.08	13.22	25/09/2017 06:35	29/09/2017 06:10
Ljungbyhed	0.86	56.08	13.22	29/09/2017 06:10	02/10/2017 06:50
Łódź	7.63	51.7592	19.456	25/09/2017 00:00	02/10/2017 00:00
Lublin	7.16	51.2465	22.5684	25/09/2017 00:00	02/10/2017 00:00
Medgidia	3.39	44.25	28.2833	07/09/2017 00:00	07/10/2017 00:00
Milano	1.09	45.473056	9.2225	25/09/2017 00:00	02/10/2017 00:00
Milano	2.49	45.473056	9.2225	29/09/2017 00:00	02/10/2017 00:00
Milano	2.5	45.473056	9.2225	29/09/2017 00:00	02/10/2017 00:00
Milano	6.3	45.473056	9.2225	02/10/2017 00:00	02/10/2017 00:00
Milano	3.6	45.473056	9.2225	02/10/2017 00:00	03/10/2017 00:00
Milano	3.5	45.473056	9.2225	03/10/2017 00:00	04/10/2017 00:00
Milano	< 1.70	45.473333	9.222778	05/10/2017 00:00	06/10/2017 00:00
Milano	< 0.62	45.473333	9.222778	06/10/2017 00:00	09/10/2017 00:00
Mircea Voda	3.1	44.2833	28.1667	05/09/2017 00:00	05/10/2017 00:00
Miskolc	14.6	48.1035	20.7784	29/09/2017 00:00	05/10/2017 00:00
Mochovce	5.78	48.2638	18.4569	25/09/2017 00:00	05/10/2017 00:00

Location	Measured Value (mBq/m^3)	Latitude	Longitude	Start Sampling [UTC]	End Sampling [UTC]
Mol (SCK-CEN)	< 1.7	51.2171	5.0904	29/09/2017 07:00	30/09/2017 07:00
Mol (SCK-CEN)	< 1.4	51.2171	5.0904	30/09/2017 07:00	01/10/2017 07:00
Mol (SCK-CEN)	< 1.2	51.2171	5.0904	01/10/2017 07:00	02/10/2017 07:00
Mol (SCK-CEN)	< 0.5	51.2171	5.0904	02/10/2017 07:00	03/10/2017 07:00
Monaco	0.0014	43.7326	7.4242	25/09/2017 10:00	02/10/2017 10:00
Monaco	0.082	43.7326	7.4242	02/10/2017 10:00	09/10/2017 10:00
Murmansk	<LD	68.958	33.083	25/09/2017 00:00	02/10/2017 00:00
Murmansk	0,0316	68.958	33.083	02/10/2017 00:00	09/10/2017 00:00
Narva-Joesuu	0.0107	59.4625	28.045	26/09/2017 00:00	03/10/2017 00:00
Narva-Joesuu	0.11	59.4625	28.045	03/10/2017 00:00	10/10/2017 00:00
Nicosia	0.0461	35.167	33.367	02/10/2017 00:00	02/10/2017 00:00
Nicosia	0.25	35.167	33.367	03/10/2017 00:00	13/10/2017 00:00
Nižná	9.06	48.5176	17.7206	27/09/2017 00:00	04/10/2017 00:00
North. Arkhangelsk. Severodvinsk	< MDA	64.5401	40.5433	25/09/2017 00:00	06/10/2017 00:00
North-West. Murmansk	< MDA	68.9792	33.0925	25/09/2017 00:00	06/10/2017 00:00
Novogornyy	18	55.633	60.787	26/09/2017 00:00	01/10/2017 00:00
Novovoronezh NPP	0,43	51.265611	39.211839	26/09/2017 00:00	02/10/2017 00:00
Novovoronezh NPP	0,1	51.265611	39.211839	02/10/2017 00:00	07/10/2017 00:00
Nový Tekov	3.99	48.25	18.5166	20/09/2017 00:00	04/10/2017 00:00
NPP Bohunice 1	10.52	48.4944	17.6819	27/09/2017 00:00	04/10/2017 00:00
NPP Bohunice 2	8.98	48.4944	17.6819	27/09/2017 00:00	04/10/2017 00:00
NPP Bohunice 3	9.8	48.4944	17.6819	27/09/2017 00:00	04/10/2017 00:00
NPP Bohunice 4	8.32	48.4944	17.6819	27/09/2017 00:00	04/10/2017 00:00
NPP Bohunice 5	10.99	48.4944	17.6819	27/09/2017 00:00	04/10/2017 00:00
NPP Bohunice 6	2.78	48.4944	17.6819	25/09/2017 00:00	02/10/2017 00:00
Obninsk	<LD	55.117	36.59	02/10/2017 00:00	06/10/2017 00:00
Odesa	45,000	46.3846	30.7433	28/09/2017 00:00	30/09/2017 00:00
Ørland	0.074	63.69	9.61	25/09/2017 00:00	02/10/2017 00:00
Ørland	0.213	63.69	9.61	02/10/2017 00:00	03/10/2017 00:00
Ørland	0.003	63.69	9.61	03/10/2017 00:00	09/10/2017 00:00
Østerås	0.186	59.94	10.6	25/09/2017 00:00	02/10/2017 00:00
Østerås	0.033	59.94	10.6	02/10/2017 00:00	03/10/2017 00:00
Østerås	< 0.055	59.94	10.6	04/10/2017 00:00	06/10/2017 00:00
Østerås	< 0.005	59.94	10.6	06/10/2017 00:00	09/10/2017 00:00

Location	Measured Value (mBq/m^3)	Latitude	Longitude	Start Sampling [UTC]	End Sampling [UTC]
Ostrava	3.8	49.833	18.283	25/09/2017 06:00	02/10/2017 06:00
Ostrava	40,000	49.833	18.283	02/10/2017 06:00	03/10/2017 15:00
Ostrava	< 0.15	49.833	18.283	04/10/2017 15:00	05/10/2017 06:30
Ostrava	< 0.5	49.833	18.283	05/10/2017 06:30	05/10/2017 14:30
Ostrava	< 0.26	49.833	18.283	05/10/2017 14:30	06/10/2017 06:00
Paks	13.5	46.6061	18.8547	25/09/2017 00:00	02/10/2017 00:00
Paks	49.4	46.6061	18.8547	30/09/2017 00:00	02/10/2017 00:00
Pečeňady	11.88	48.4763	17.7181	27/09/2017 00:00	04/10/2017 00:00
Perugia	0.91	43.081944	12.338056	29/09/2017 00:00	02/10/2017 00:00
Perugia	6.2	43.081944	12.338056	02/10/2017 00:00	03/10/2017 00:00
Plzeň	0.62	49.73	13.37	26/09/2017 09:00	03/10/2017 09:00
Praha	15,000	50.067	14.45	29/09/2017 06:45	02/10/2017 16:35
Praha	1.6	50.067	14.45	02/10/2017 16:40	02/10/2017 20:25
Praha	1.1	50.067	14.45	02/10/2017 20:25	03/10/2017 08:10
Praha	< 0.04	50.067	14.45	03/10/2017 08:10	03/10/2017 15:00
Praha	< 0.05	50.067	14.45	04/10/2017 07:55	05/10/2017 08:05
Praha	< 0.012	50.067	14.45	05/10/2017 08:05	06/10/2017 06:40
Praha	< 0.015	50.067	14.45	06/10/2017 06:40	07/10/2017 10:30
Rahiv	2.6	48.0552	24.2135	27/09/2017 00:00	29/09/2017 00:00
Retz	13,000	48.754863	15.950598	25/09/2017 18:55	02/10/2017 11:43
Risø	<MDA	55.693357	12.09705	26/09/2017 00:00	03/10/2017 00:00
Rivno Npp	1.24	51.3294	25.8939	29/09/2017 00:00	03/10/2017 00:00
Roskilde	0.0008	55.69	12.1	26/09/2017 00:00	02/10/2017 00:00
Roskilde	<MDA	55.69	12.1	02/10/2017 00:00	10/10/2017 00:00
Rostov NPP	4,41	47.604	42.373894	29/09/2017 00:00	13/10/2017 00:00
Saligny	4,54	44.2833	28.0833	07/09/2017 00:00	03/10/2017 00:00
Saligny	4.54	44.2833	28.0833	07/09/2017 00:00	03/10/2017 00:00
Salzburg	< 9.6E-03	47.790951	13.052636	25/09/2017 08:30	02/10/2017 08:20
Sanok	6.52	49.555	22.2061	25/09/2017 00:00	02/10/2017 00:00
Sarajevo	4.76	43.8638889	18.4175	22/09/2017 00:00	02/10/2017 00:00
Sarajevo	3.17	43.8638889	18.4175	02/10/2017 00:00	09/10/2017 00:00
Seimeni	5,34	44.4018	28.0876	06/09/2017 00:00	04/10/2017 00:00
Seimeni	5.34	44.4018	28.0876	06/09/2017 00:00	04/10/2017 00:00
Severodvinsk	<LD	64.566	39.85	25/09/2017 00:00	06/10/2017 00:00
Site of Kozloduy NPP	58.9	43.74611	23.77056	15/09/2017 00:00	02/10/2017 00:00
Skibotn	< 0.003	69.37	20.3	25/09/2017 00:00	02/10/2017 00:00
Skibotn	0.094	69.37	20.3	02/10/2017 00:00	09/10/2017 00:00
Smolensk NPP	<LD	54.1658	33.233371	01/09/2017 00:00	30/09/2017 00:00
Smolensk NPP	<LD	54.1658	33.233371	01/10/2017 00:00	31/10/2017 00:00
Snovsk (Shtors)	0.1	51.8159	31.9582	29/09/2017 00:00	01/10/2017 12:00
Sola	< 0.001	58.88	5.64	22/09/2017 00:00	29/09/2017 00:00
Sola	< 0.002	58.88	5.64	29/09/2017 00:00	03/10/2017 00:00
Sola	< 0.002	58.88	5.64	03/10/2017 00:00	06/10/2017 00:00
South Kursk Kurchatov city	< MDA	51.7373	36.1874	29/09/2017 00:00	04/10/2017 00:00

Location	Measured Value (mBq/m^3)	Latitude	Longitude	Start Sampling [UTC]	End Sampling [UTC]
South-Ukraine NPP	29,000	47.81667	31.21667	29/09/2017 00:00	03/10/2017 00:00
St Petersburg	0,115	59.938	30.335	02/10/2017 00:00	06/10/2017 00:00
Stockholm (A3)	< 0.034	59.39	17.96	29/09/2017 15:44	30/09/2017 19:44
Stockholm (A3)	6.56	59.39	17.96	30/09/2017 19:44	01/10/2017 23:44
Stockholm (A3)	14.8	59.39	17.96	01/10/2017 23:44	03/10/2017 03:44
Stockholm (A3)	< 0.044	59.39	17.96	04/10/2017 07:44	05/10/2017 11:44
Stockholm (SEP63)	0.032	59.39	17.96	30/09/2017 08:42	01/10/2017 08:42
Stockholm (SEP63)	17,000	59.39	17.96	01/10/2017 08:42	02/10/2017 08:42
Stockholm (SEP63)	9.8	59.39	17.96	02/10/2017 08:42	03/10/2017 08:42
Straß-Spielfeld	9.4	46.725903	15.624754	25/09/2017 08:15	02/10/2017 10:35
Sukhobuzimsky	0,2076	56.514167	93.273996	06/10/2017 00:00	07/10/2017 00:00
Svanhovd	< 0.010	69.45	30.04	13/10/2017 00:00	16/10/2017 00:00
Szczecin	0.36	53.4285	14.5528	25/09/2017 00:00	02/10/2017 00:00
Tajná	4.23	48.2666	18.3666	20/09/2017 00:00	04/10/2017 00:00
Topalu	2.94	44.4323	26.1063	06/09/2017 00:00	06/10/2017 00:00
Toravere	<MDA	58.2644	26.4617	25/09/2017 00:00	02/10/2017 00:00
Toravere	0.21	58.2644	26.4617	02/10/2017 00:00	09/10/2017 00:00
Torun	9.93	53.0174	18.6571	25/09/2017 00:00	02/10/2017 00:00
Trakovice	8.88	48.4333	17.6999	27/09/2017 00:00	04/10/2017 00:00
Trino	1.14	45.311944	8.296111	29/09/2017 00:00	02/10/2017 00:00
Tsimlyansk	13,6	47.63	42.12	26/09/2017 00:00	01/10/2017 00:00
Udine	12.5	46.063333	13.235833	29/09/2017 00:00	02/10/2017 00:00
Udine	49.1	46.063333	13.235833	02/10/2017 00:00	03/10/2017 00:00
Udine	54.3	46.063333	13.235833	03/10/2017 00:00	03/10/2017 00:00
Udine	30,000	46.063333	13.235833	03/10/2017 00:00	04/10/2017 00:00
Udine	3.3	46.063333	13.235833	05/10/2017 00:00	06/10/2017 00:00
Udine	< 1.10	46.063333	13.235833	06/10/2017 00:00	07/10/2017 00:00
Udine	< 1.50	46.063333	13.235833	07/10/2017 00:00	09/10/2017 00:00
Umeå	< 0.005	63.85	20.34	25/09/2017 11:01	02/10/2017 08:41
Ural Region. Ekaterinburg	< MDA	60.6057	56.8389	26/09/2017 00:00	05/10/2017 00:00
Ústí Nad Labem	4.35	50.667	14.033	26/09/2017 11:00	04/10/2017 09:00
Veľké Kostoľany 1	9.54	48.5176	17.7206	27/09/2017 00:00	04/10/2017 00:00
Veľké Kostoľany 2	9.76	48.5176	17.7206	27/09/2017 00:00	04/10/2017 00:00
Vercelli	1.25	45.31	8.407778	29/09/2017 00:00	05/10/2017 00:00
Verona	5.58	45.426667	10.991944	29/09/2017 00:00	02/10/2017 00:00
Verona	19.1	45.426667	10.991944	02/10/2017 00:00	03/10/2017 00:00
Verona	< 1.93	45.426944	10.992222	05/10/2017 00:00	06/10/2017 00:00

Location	Measured Value (mBq/m^3)	Latitude	Longitude	Start Sampling [UTC]	End Sampling [UTC]
Vicenza	8.4	45.545833	11.561667	29/09/2017 00:00	02/10/2017 00:00
Vicenza	25.2	45.545833	11.561667	02/10/2017 00:00	03/10/2017 00:00
Vicenza	< 3.10	45.426944	10.992222	05/10/2017 00:00	06/10/2017 00:00
Viksjofjell	< 0.002	69.62	30.81	24/09/2017 00:00	01/10/2017 00:00
Visby	< 0.01	57.61	18.32	25/09/2017 06:00	28/09/2017 06:00
Visby	5.16	57.61	18.32	28/09/2017 06:00	02/10/2017 06:30
Volgograd (RU)	19	48.7	44.5	26/09/2017 00:00	01/10/2017 00:00
Warszawa	4.09	52.2297	21.0122	25/09/2017 00:00	02/10/2017 00:00
Wien 22	13.2	48.256525	16.482973	25/09/2017 09:13	02/10/2017 09:10
Wien 22	46,000	48.256525	16.482973	02/10/2017 09:10	03/10/2017 09:22
Wien 22	< 0.1	48.256525	16.482973	04/10/2017 09:10	05/10/2017 08:47
Wien 22	< 0.2	48.256525	16.482973	05/10/2017 08:51	06/10/2017 08:54
Wien 22	8,000	48.256525	16.482973	02/10/2017 09:05	09/10/2017 08:55
Wrocław	3.03	51.1079	17.0385	25/09/2017 00:00	02/10/2017 00:00
Zagreb	< MDA	45.815398	15.966567	01/09/2017 00:00	29/09/2017 00:00
Zagreb	0.0341	45.815399	15.966568	09/10/2017 00:00	10/10/2017 00:00
Zaporizhzhya Npp	40,000	47.5067	34.5851	29/09/2017 00:00	03/10/2017 00:00
Zielona Góra	3.99	51.9356	15.5062	25/09/2017 00:00	02/10/2017 00:00
Ukraine	3.9	47.820885	31.186263	22/09/2017 00:00	29/09/2017 00:00
Ukraine	23,000	47.49978	34.57049	25/09/2017 00:00	02/10/2017 00:00
Ukraine	18,000	47.514744	34.594483	25/09/2017 00:00	02/10/2017 00:00
Ukraine	30,000	47.486322	34.416862	25/09/2017 00:00	02/10/2017 00:00
Ukraine	36,000	47.434942	34.382228	25/09/2017 00:00	02/10/2017 00:00
Ukraine	23,000	47.804651	31.259567	26/09/2017 00:00	03/10/2017 00:00
Ukraine	29,000	47.907871	31.31512	26/09/2017 00:00	03/10/2017 00:00
Ukraine	14,000	48.106339	31.283112	26/09/2017 00:00	03/10/2017 00:00
Ukraine	40,000	47.48135	34.57228	26/09/2017 00:00	03/10/2017 00:00
Ukraine	27,000	47.49191	34.63695	26/09/2017 00:00	03/10/2017 00:00
Ukraine	36,000	47.249982	35.710817	26/09/2017 00:00	03/10/2017 00:00
Ukraine	24,000	47.603631	31.20605	27/09/2017 00:00	04/10/2017 00:00
Ukraine	17,000	47.768059	31.311445	27/09/2017 00:00	04/10/2017 00:00
Ukraine	30,000	47.52209	34.655161	27/09/2017 00:00	04/10/2017 00:00
Ukraine	27,000	47.481892	34.504167	27/09/2017 00:00	04/10/2017 00:00
Ukraine	24,000	47.81968	31.223832	28/09/2017 00:00	05/10/2017 00:00
Ukraine	24,000	47.803507	30.888264	28/09/2017 00:00	05/10/2017 00:00
Ukraine	15,000	47.556679	34.401924	28/09/2017 00:00	05/10/2017 00:00
Ukraine	1.3	47.480731	34.756507	28/09/2017 00:00	05/10/2017 00:00
Ukraine	0.0503	46.15	8.95	02/10/2017 00:00	02/10/2017 23:59
Ukraine	1.02	51.4381	25.8161	28/09/2017 00:00	07/10/2017 00:00
Ukraine	1.05	51.3106	26.0929	28/09/2017 00:00	07/10/2017 00:00
Ukraine	0.914	51.3228	25.9179	28/09/2017 00:00	07/10/2017 00:00
Ukraine	1.2	51.3755	26.0282	28/09/2017 00:00	07/10/2017 00:00
Ukraine	1.14	51.2581	26.0643	28/09/2017 00:00	07/10/2017 00:00

Location	Measured Value (mBq/m^3)	Latitude	Longitude	Start Sampling [UTC]	End Sampling [UTC]
Ukraine	1.26	51.3418	25.9675	28/09/2017 00:00	07/10/2017 00:00
Ukraine	0.953	51.4119	25.8908	28/09/2017 00:00	07/10/2017 00:00
Ukraine	1.23	51.3363	25.8548	28/09/2017 00:00	07/10/2017 00:00
Ukraine	1.19	51.3251	25.8897	28/09/2017 00:00	07/10/2017 00:00
Ukraine	1.13	51.3176	25.8768	28/09/2017 00:00	07/10/2017 00:00
Ukraine	1.39	51.36	25.9199	28/09/2017 00:00	07/10/2017 00:00
Ukraine	1.5	46.6406	15.6958	30/09/2017 10:00	05/10/2017 10:00
Ukraine	1.92	46.15	8.95	03/10/2017 00:00	03/10/2017 23:59
Ukraine	0.498	46.15	8.95	05/10/2017 00:00	05/10/2017 23:59

LD : detection limit

MDA : minimum detection activity